MERT TOPCUOĞLU

SYNTHESIZE AND PHOTOCATALYTIC APPLICATIONS OF TITANIUM DIOXIDE AND MAGNETIC NANOPARTICLES CONTAINING HIGH SULFUR CONTENT POLYMERIC COMPOSITES

THE GRADUATE SCHOOL OF NATURAL AND APPLIED SCIENCES
OF
ATILIM UNIVERSITY

MERT TOPCUOĞLU

A MASTER OF SCIENCE THESIS
IN
THE DEPARTMENT OF CHEMICAL ENGINEERING

JANUARY 2022

ATILIM UNIVERSITY 2022

SYNTHESIZE AND PHOTOCATALYTIC APPLICATIONS OF TITANIUM DIOXIDE AND MAGNETIC NANOPARTICLES CONTAINING HIGH SULFUR CONTENT POLYMERIC COMPOSITES

A THESIS SUBMITTED TO
THE GRADUATE SCHOOL OF NATURAL AND APPLIED SCIENCES
OF
ATILIM UNIVERSITY

BY

MERT TOPCUOĞLU

IN PARTIAL FULFILLMENT OF THE REQUIREMENTS
FOR
THE DEGREE OF MASTER OF SCIENCE
IN
THE DEPARTMENT OF CHEMICAL ENGINEERING

JANUARY 2022

Approval of the Graduate School of Natural and Applied Sciences, Atılım University.

Prof. Dr. Ender Keskinkılıç
Director

I certify that this thesis satisfies all the requirements as a thesis for the degree of **Master of Science in Chemical Engineering and Applied Chemistry at Atılım University**.

Prof. Dr. Şeniz Özalp Yaman
Head of Department

This is to certify that we have read the thesis "SYNTHESIZE AND PHOTOCATALYTIC APPLICATIONS OF TITANIUM DIOXIDE AND MAGNETIC NANOPARTICLES CONTAINING HIGH SULFUR CONTENT POLYMERIC COMPOSITES" submitted by MERT TOPCUOĞLU and that in our opinion it is fully adequate, in scope and quality, as a thesis for the degree of Master of Science.

Prof. Dr. Atilla Cihaner
Co-Supervisor

Prof. Dr. Murat Kaya
Supervisor

Examining Committee Members:

Assoc. Prof. Dr. Merve İçli Özkut
Chemistry Department, Ankara University

Prof. Dr. Murat Kaya
Chemical Engineering Department, Atılım University

Asst. Prof. Dr. Salih Ertan
Chemical Engineering Department, Atılım University

Date: *24.01.2022*

I hereby declare that all information in this document has been obtained and presented in accordance with academic rules and ethical conduct. I also declare that, as required by these rules and conduct, I have fully cited and referenced all material and results that are not original to this work.

Name, Last Name: Mert Topcuoğlu

Signature:

ABSTRACT

SYNTHESIZE AND PHOTOCATALYTIC APPLICATIONS OF TITANIUM DIOXIDE AND MAGNETIC NANOPARTICLES CONTAINING HIGH SULFUR CONTENT POLYMERIC COMPOSITES

Topcuoğlu, Mert

M.Sc., Department of Chemical Engineering

Supervisor: Prof. Dr. Murat Kaya

Co-Supervisor: Prof. Dr. Atilla Cihaner

January 2022, 53 pages

Sulfur is one of the most abundant elements in nature. It is not toxic but is a flammable solid even though it is stored outdoors. Approximately 70 million tons of sulfur is obtained as a by-product from oil refineries every year but the use of this huge amount of sulfur is very limited. Therefore, it is very important to convert elemental sulfur into valuable products like polymers and ensure the use of large quantities in industry.

In this study, the synthesis of new high sulfur polymeric materials using vegetable fatty acid and their usage as a support material in the preparation of photocatalyst for methylene blue removal is aimed. For this purpose, copolymerization of elemental sulfur and fatty acid, linolenic acid (LnA), was carried out by reverse vulcanization method. The photocatalytic activities of the prepared polysulfur copolymers were tested in the degradation of methylene blue under a solar simulator for comparison study. Then, polysulfur copolymer was prepared again by adding magnetic nanoparticles and titanium dioxide nanoparticles. The photocatalytic activity of the

resulting composite material, poly(S-r-FA)-TiO_2-MNP, was examined in the same reaction. Also, stability of the composite material was carried out. The characterization of the prepared materials was carried out using SEM, TEM, EDX, FTIR, and NMR. The decrease in dye concentration was followed by UV-Vis spectrometry.

Keywords: Sulfur, inverse vulcanization, photocatalyst, titanium dioxide, magnetic nanoparticle

ÖZ

TİTANYUM DİOKSİT VE MANYETİK NANOPARÇACIK İÇEREN YÜKSEK KÜKÜRT İÇERİKLİ POLİMERİK KOMPOZİTLERİN SENTEZİ VE FOTOKATALİTİK UYGULAMALARI

Topcuoğlu, Mert
Yüksek Lisans, Kimya Mühendisliği
Tez Yöneticisi: Prof. Dr. Murat Kaya
Ortak Tez Yöneticisi: Prof. Dr. Atilla Cihaner

Ocak 2022, 53 sayfa

Doğada en çok bulunan elementlerden birisi olan kükürt zehirli olmayıp açık havada depolanmasına rağmen yanıcı bir katıdır. Her yıl petrol rafinerilerinden yan ürün olarak yaklaşık 70 milyon ton kükürt elde edilmesine rağmen bu devasa miktardaki kükürtün kullanım alanı çok sınırlıdır. Bu nedenle elementel kükürtün katma değeri yüksek ürünlere (polimerler gibi) dönüştürülmesi ve endüstride büyük miktarlarda kullanım bulmasını sağlamak önemlidir.

Bu projede bitkisel yağ asitleri kullanarak yeni yüksek kükürt içerikli polimerik malzemelerin sentezi ve metilen mavisi gideriminde kullanılacak fotokatalizör için destek malzemesi olarak kulanımı hedeflenmiştir. Bu amaçla ters vulkanizasyon yöntemi ile elemental kükürt ve yağ asiti, linolenik asit (LnA), kopolimerizasyonu gerçekleştirilmiştir. Elde edilen polikükürt kopolimerin fotokatalitik etkinliği solar simulator altında metilen mavisinin bozunmasında denenmiştir. Daha sonra polikükürt kopolimere manyetik nanoparçacık ve titanyum dioksit nanoparçacık eklenerek tekrar hazırlanmış ve kompozit malzeme, poly(S-r-FA)-TiO_2-MNP, elde

edilerek fotokatalitik etkinliği incelenmiştir. Daha sonra kompozit malzeme ile kararlılık çalışması yapılmıştır. Hazırlanan mazlemelerin karakterizasyonları SEM, TEM, EDX, FTIR ve NMR kullanılarak gerçekleştirilmiştir. Boya derişimindeki azalma UV-Vis spektrometresi ile takip edilmiştir.

Anahtar Kelimeler: Kükürt, ters vulkanizasyon, fotokatalizör, titanyum dioksit, manyetik nanoparçacık.

To my family…

ACKNOWLEDGMENTS

First of all, I owe my deepest respect and dept of gratitude to my supervisor, Prof. Dr. Murat Kaya and my co-supervisor Prof. Dr. Atilla Cihaner for their endless support, mentorship, their patience and sincerity. I would not have been able to carry out these studies without their support during the academic research and writing of this thesis.

I shall also thank to rest of my thesis committee Assoc. Prof. Dr. Merve İçli Özkut and Asst. Prof. Dr. Salih Ertan for helping me make progress in my thesis with their positive feedback and suggestive questions and comments.

Furthermore, I would also like to express my appreciation to my colleagues Tuğçe Gültan Gürbüz, Zuhal Selvi Vanlı Güner, Vahide Selen Yaman, Fırat Ayan and Mücahit Cihan Terzi and dear friends in my laboratory group Ezgi Karakoç, Hasan Berk, Burcu Balcı and Büşra Kesimal for their helps and valuable time shared with me. Also, I would like to take this occasion to thank you all members of the Atılım Optoelectronic Materials and Solar Energy Laboratory (ATOMSEL) research group and the Chemical Engineering Department of the Atılım University

I would like to express my endless thanks and gratitude to my parents, Mehmet and Derya Topcuoğlu who brought me up to this age and care about me, and my brother Nuri Topcuoğlu, for making me live this precious and beautiful life.

I would also like to acknowledge and thank the Scientific and Technical Research Council of Turkey (TÜBİTAK) for the financial support of the (Grant Number: 118Z343).

TABLE OF CONTENT

LIST OF TABLES

LIST OF FIGURES

LIST OF SYMBOLS/ABBREVIATIONS

$CoFe_2O_4$	Cobalt Ferrite
d-$CHCl_3$	Deuterated Chloroform
d-DMSO	Deuterated Dimethyl Sulfoxide
EDX	Energy Dispersive X-ray Spectrometer
FA	Fatty Acid
FE-SEM	Field Emission Scanning Electron Microscope
FTIR	Fourier Transferred Infrared Spectroscopy
^{1}H NMR	Proton Nuclear Magnetic Resonance Spectroscopy
LnA	Linolenic Acid
MB	Methylene Blue
MNP	Magnetic Nanoparticle
Poly(S-r-FA)	Poly (sulfur-random-fatty acid)
Poly(S-r-LnA)	Poly (sulfur-random-linolenic acid)
S_8	Eight-Member Ring Shaped Elemental Sulfur
SiO_2	Silica
TEM	Transmission Electron Microscopy
TiO_2	Titanium Dioxide
UV-Vis	Ultraviolet-Visible

CHAPTER 1

1 INTRODUCTION

1.1 Sulfur

Sulfur is an element identified by the ‘S’ letter and it is placed in the 3rd period, 6A group, and ‘p’ block in the periodic table.

It is an element found in abundance in nature in solid form at the standard temperature and pressure. This bright yellow-colored element has a molecular mass of 32.06 g per mole and the density of the sulfur is 2.07 g per cubic centimeter at room temperature.

Figure 1.1 Solid sulfur

Sulfur can be melted at 120℃ or 293.15 K at standard atmospheric pressure. The bright yellow color of the sulfur is turned into honey-yellow after it is liquefied. In addition to this, the boiling point of the sulfur is 445°C or 713.15 K and the color turns dark red-brown. The density of molten sulfur decreases from 1.802 to 1.573 gram per cubic centimeter at atmospheric pressure while the temperature is increasing from 120ºC to 440ºC respectively [1].

In nature, sulfur is found in an eight-member ring shape solid compound. It is only necessary to melt it to open the ring shape of sulfur and the molten sulfur is polymerized by itself. However, after cooling the sulfur slowly, it is possible to obtain the S_8 ring structure back with the same temperature-related changes of the physical properties [2].

1.2 Sulfur Resources

There is a current global problem of excess sulfur originating from the world's petrochemical industry. Sulfur is produced as a waste byproduct from the purification processes of crude oil and gas reserves. The sulfur atoms, sulfur dioxide (SO_2), and hydrogen sulfide (H_2S) in organosulfur compounds are separated from the source and by hydrodesulfurization process; they are converted to elemental sulfur (S_8) [3, 4]. Around 70 million tons of elemental sulfur were produced annually in 2016 by this process, and it was expected that this amount will increase as long as the energy need of the world and consumption of sulfur-containing oil increases [4]. In 2019, this expectation was met and sulfur production rose around to 79 million tons per year [5].

Figure 1.2 Sulfur stockpiles that are produced as a byproduct of petroleum refinery [3].

Coincidentally, sulfur, the 16th element of the periodic table, is the 16th most abundant element in nature. As with most of the elements, sulfates (SO_4^{-2}) and

sulfides (S^{-2}), combined forms of sulfur minerals, are more common than elemental sulfur (S^8). One of the most important mineral sources in terms of sulfur is sulfides, especially pyrites (iron sulfide, FeS_2; also a term for copper sulfide). They are seen as the most common source of sulfur for sulfuric acid production., except for elemental sulfur itself. Releasing sulfur dioxide, due to smelting processes of metal sulfides such as zinc, copper, and nickel is the reason for acid rains unless it is collected. However, sulfur dioxide can be used in the production of sulfuric acid. Production of "metallurgical" sulfuric acid occurs through the capture of sulfur dioxide [6].

1.3 Sulfur's Usage Areas

Sulfur has been used for centuries in a variety of applications such as medicine, fabric bleaching, making lamp wicks, formulation of gun powder, and later in the vulcanization of latex [6, 7]. In addition, sulfur is used mainly in the production of chemicals such as sulfuric acid, phosphorus sulfides, etc., and also it is used in vulcanization processes of natural or synthetic rubber [1]. Almost half of the produced sulfuric acid in the world is consumed in the production of phosphate fertilizers [6].

Many researchers have been attracted to develop new materials due to the excess sulfur overproduction with increased usage of oil and gas as a result of increased energy demand, and availability of this affordable, unused sulfur [8]. Much greater use of sulfur in the industry has been made possible by the pioneering work of Pyun et al. in recent years [9]. Since materials made from sulfur have the potential to be made in bulk at a low enough cost to make them feasible for large-scale use in Hg capture, many studies are underway to increase the use of unused elemental sulfur. Therefore, inverse vulcanized high-sulfur content polymers have received much attention recently due to their diverse applications and potentially low cost [10].

1.4 Vulcanization Process

Vulcanization is a chemical process that is used to convert natural rubber, polydiene, and elastomers (polymers), which are used in daily life as a part of various

components, e.g. tires, seals, protective gloves, etc., into cross-linked polymers to qualify different mechanical and thermal properties to the material [11]. One of the most common vulcanizing agents is sulfur that can create a bridge to cross-link polymeric chains.

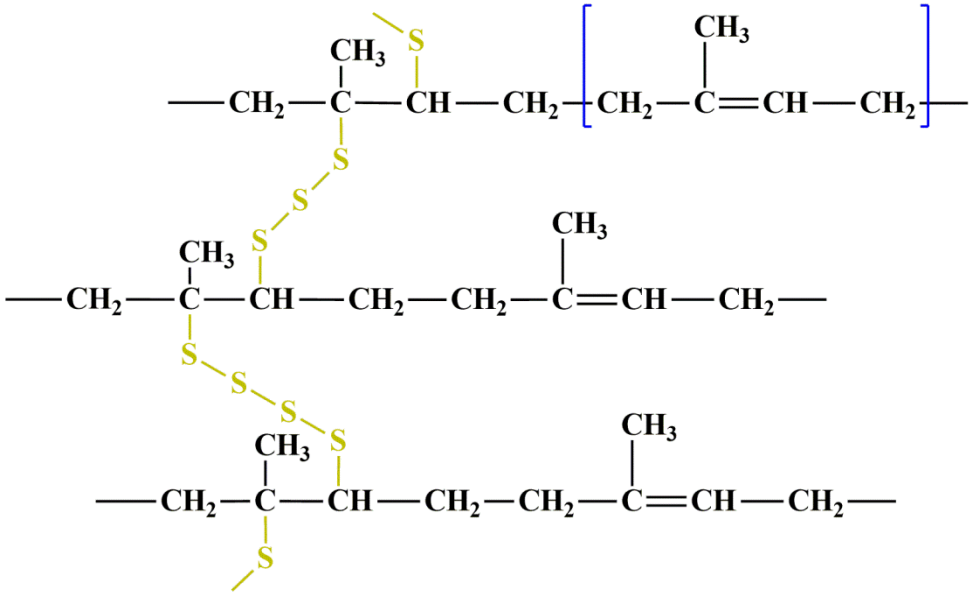

Figure 1.3 Natural rubber vulcanized by sulfur. Monomer cis 1,4 polyisoprene is shown in blue [11].

To modify the chemical and physical properties of elemental sulfur copolymerization strategies have been investigated by incorporating sulfur into polymeric materials. The stimulating work of Penczek and co-workers manifested the ability of copolymerization of S_8 anionically with propylene sulfide to form nine S–S bonds in linear polysulfides [12, 13]. Free radical copolymerization of S_8 is studied with styrene by Stillo and co-workers, which yields essentially oligomeric products if divinyl monomers were not used to balance the depolymerization process with crosslinking [14]. Tsuda and Takeda studied the copolymerization of diynes via vulcanization technique with S_8 to form regional polythiophenes [15]. Ding and Hay demonstrated intractable copolymers with increasing sulfur feed ratios with the copolymerization of cyclic disulfides with S_8 [16]. While all of these reports reveal the potential to use sulfur, these materials either form polymeric materials with limited processability and adjustability of properties or are copolymers with low degrees of sulfur.

1.5 Inverse Vulcanization Process

As it was mentioned earlier molten sulfur polymerizes itself but it is unstable without having a vulcanization or inverse vulcanization reaction and the sulfur amount is fairly low in the polymers are obtained by the vulcanization process. Therefore, inverse vulcanization is only the way to obtain stable polymers with a high fraction of sulfur (higher than 50wt%). Inverse vulcanization is providing the possibility of the production of high sulfur content polymers by crosslinking sulfur with small-molecule dienes to stabilize against depolymerization as shown in Figure 1.4. Additionally, this is a solvent-free process which makes it more beneficial in terms of economy and applicability.

Due to its limited solubility and poor compatibility with organic compounds, the processing of sulfur is challenging. In addition, the dependence of the physical and chemical properties of sulfur on the temperature makes it tough to process [17, 18]. These issues were overcome by the inverse vulcanization technique; the reaction of the active sulfur chain ends with organic dienes to produce a highly cross-linked stable polymer [9].

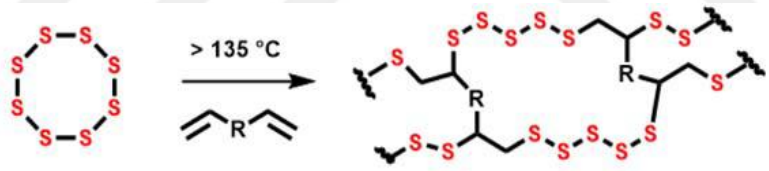

Figure 1.4 Inverse vulcanization reaction of elemental sulfur (S_8) and crosslinker, where R denotes an organic molecule with unsaturated bonds [10].

As it is said, the inverse vulcanization is a bulk free-radical copolymerization of unsaturated co-monomers in liquid sulfur [19]; nevertheless, the mechanism is complex and uncertainty remains just as in the conventional vulcanization process. Both hydrogen abstraction [20] and radical addition across the double bonds have been asserted [3, 9], and the nature of the reaction is likely to be crosslinker and temperature-dependent.

1.6 Sulfur Based Polymers

Over the past century, several studies have been conducted on the use of elemental sulfur for the production of polymeric materials. These polymeric materials have been used and benefited in various fields and the studies have been an inspiring source for subsequent researchers. Polymeric materials production from sulfur by inverse vulcanization process is firstly reported by Pyun et al. [9] who have used small diene molecules as a crosslinker to provide the stabilization of sulfur polymers such as dicyclopentadiene, which stabilize polymer but makes polymer a brittle crystalline material [17].

Synthetizing and processing methods for preparing well-defined materials with high sulfur content are largely lacking, although they are known to have some interesting properties such as high electrochemical capacities [21-32] and high refractive indices [33, 34]. In the application areas of synthesis and battery applications, high sulfur content copolymers were used by the use of various crosslinkers via inverse vulcanization process [9, 35-40]. Despite its many advantages and application, the improvement of new innovative materials made from sulfur is still very much in the preliminary stages [41].

In order to synthesize polysulfide copolymers with many different chemical and mechanical properties, the researchers used various unsaturated cross-linkers [3]. Some of these cross-linkers are divinylbenzene [42-44], 4-vinylpyridine [45], limonene [46], myrcene [47, 48], alkenyl alcohol [49], styrene , methylstyrene [50], farnesol, farnesene, dicyclopentadiene [48], 1,3-diisopropenylbenzene [9], bismaleimide [51], benzoxazine [20, 52], 1,3,5-triisopropenylbenzene [53], eugenol [54], vegetable oils (linseed oil, sunflower oil, olive oil, canola oil) [55, 56], 1,3-diethynylbenzene [57], 1,4-diphenylbutadiyne [58], diallylsulfide [47, 59] and oleylamine [60]. These related polysulfide copolymers showed some interesting chemical, optical and mechanical properties due to the high content of sulfur.

Palladium is a valuable heavy metal that is used as a catalyst in a variety of organic transformations [61, 62], and it is desired to recover palladium from waste streams. Also, palladium has been qualified as a pollutant that percolated from catalytic

converters by automobile exhaust [63]. So that, recovery of palladium is important due to environmental and economic factors and it is useful to know that polysulfides are used in the processes. Also, mercury is a highly toxic heavy metal that is encountered in a variety of industrial activities including coal burning, oil and gas refining, and artisanal and small-scale gold mining [64-66]. Mercury exposure can cause some serious health problems, including debilitating neurological and embryotoxic effects [67]. For this reason, the removal of mercury pollution is essential in protecting human health and the environment. Therefore, the effects of polysulfides in removing the highly toxic mercury from water were emboldening [46].

In the literature review, no polysulfide copolymer was found which is in used as photocatalytic in dye removal methods. It is hoped that the copolymers produced in this study will be a pioneer in this field and will guide future studies.

1.7 Renewable Alkene Resources

About 80% of the world's oil production comes from plants and the remaining 20% is from animal fats. This information adds another plus to the use of renewable vegetable oils such as oleic acid (OA), linoleic acid (LA), and linolenic acid (LnA) in polymer production [68]. It was mentioned that polysulfide materials are used in environmental remediation processes. Sustainable sources of materials used in the synthesis of useful and functional materials such as polysulfide are of vital importance for the production of these materials in the future. Also, searching for renewable crosslinkers for polysulfides will enable the development of polymeric sulfur materials for bulk applications. The preparation of these polymers by copolymerization of sulfur and renewable alkenes such as terpenes and triglycerides provides further benefits to the environment [3].

In this study linolenic acid was used as renewable alkene crosslinker (fatty acid) in the synthesize of polysulfide copolymers.

1.7.1 Linolenic Acid

Linolenic acid (LnA) is a polyunsaturated fatty acid with 3 double bonds in the main carbon chain. Hempseed, chia, perilla, linseed oil, canola, and soybeans are some of the LnA resources.

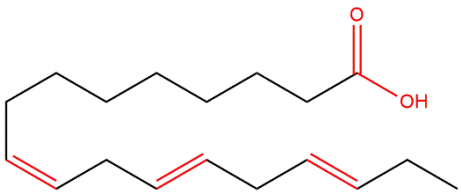

Figure 1.5 Chemical structure of linolenic acid

1.8 Titanium Dioxide

Titanium dioxide (TiO_2) is a well-known photocatalyst with good stability, low cost, and operability in a wide pH range. It is a high efficient photocatalyst under UV light for the degradation of contaminants [69]. Since it has been observed to be active in the ultra violet band, titanium dioxide (TiO_2) has been documented to be an essential photocatalyst. A substance must be able to change its oxidation state without decomposing to be regarded as a useful and efficient photocatalyst. It is affordable when compared to other water treatment materials, and it can be easily made in a laboratory [70]. TiO_2 performs an oxidation state transition without breakdown, which is a crucial feature of a good photo catalyst [71, 72]. Some of the features that make it so prone to use are the greatly increased surface area, faster rates, non-toxic nature, biocompatibility, and ease of preparation. Therefore, titanium dioxide in the form of nanostructures is becoming a more preferred option in the field of photocatalysis [73].

The five-step path of heterogeneous photocatalysis in the presence of titanium dioxide is as follows:

i. Mass transfer to the photocatalyst surface of the molecules for degradation [74]
ii. Adsorption of degradable molecules onto active sites of titanium dioxide and photoexcitation of valence band electrons [75]

iii. Adsorbed molecules' photocatalytic degradation

iv. Desorption of the products that are produced by degradation from the surface

v. Mass transfer of products from the surface of titanium dioxide photocatalyst

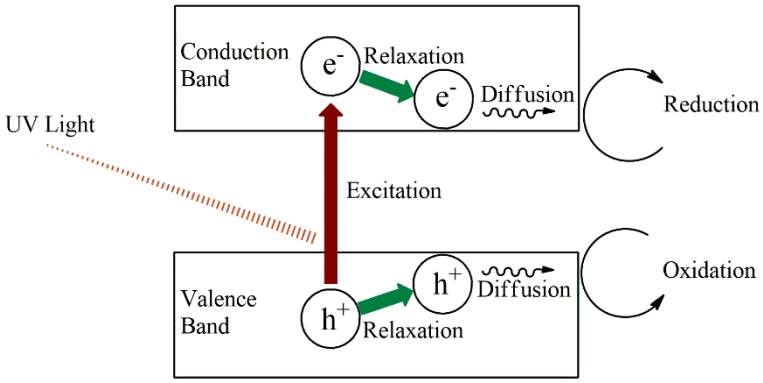

Figure 1.6 Schematic representation of photogenerated charge carriers, hole and electron, formation

The generation of photogenerated charge carriers, which are holes and electrons, occurs when UV light corresponding to the band gap is absorbed by TiO_2 (Fig. 1.8). Photogenerated holes (represented as h^+ in Figure 1.8) in the valence band then diffuse to the surface of TiO_2, where they combine with water molecules which are adsorbed to produce hydroxyl radicals ($^{\bullet}OH$). On the TiO_2 surface, adjacent organic molecules are oxidized by photogenerated holes and hydroxyl radicals. Meanwhile, conduction band electrons (represented as e^- in Figure 1.8) are participating in reduction processes, which form superoxide radical anions ($O_2^{\bullet-}$) when they combine with oxygen molecules in the air [76].

Due to the possibility of its reuse as a catalyst and heterogeneous nature, it has been studied comprehensively. Doped or undoped TiO_2 nanopowders increase the likelihood of catalyst contact if suspended in water. However, the main disadvantage of this process, phase separation requiring multiple steps, is an expensive process for large-scale use [77].

The various types of pollutants that can be remediated using TiO_2, their negative effects on human and animal health, the mechanisms by which TiO_2 is capable of performing photodegradation on the various pollutants, the beneficial properties that

it possesses, its limitations, and the various modifications and improvements made to it to improve its efficiency and performance were all examined.

In literature research the use of TiO_2 is given with some polymers such as polyaniline [78, 79] or coating MNP is commonly advised to increase the effect and try to get rid of negative effects such as phase separation requirement.

1.9 Magnetic Nanoparticle

Magnetic nanoparticles (MNP) have been intensively studied in recent decades in the discovery of innovative nanostructures to be used in environmental applications in water purification for human consumption, contaminated water remediation, and industrial or residential effluents [80-83].

Maghemite (γ-Fe_2O_3) and magnetite (Fe_3O_4), in particular, are iron oxide-based MNPs with appealing magnetic characteristics [84]. Since their magnetic features, they can be separated subsequently well into the application of a magnetic field, therefore they can be promising agents in water purification.

The coating of MNP is advised in photocatalysis applications in water treatment and environmental remediation to generate core-shell structures by including a magnetic core, avoiding detrimental effects during the application. Mesoporous silica is among the most desirable coating materials. It provides a large surface area including well pore size and shape, minimizing the possibility of aggregation while having little impact on the core's magnetization [81]. In this study, magnetic cobalt ferrite ($CoFe_2O_4$) impregnated with mesoporous silica [85] was used as MNP.

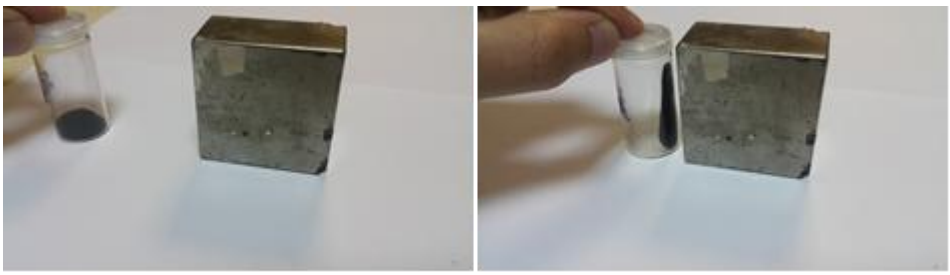

Figure 1.7 Cobalt ferrite ($CoFe_2O_4$) impregnated with mesoporous silica used as MNP

Using magnetic core-shell-shell structures, enabling separation of the photocatalyst out from liquid using an external magnetic field can be considerably facilitated. Furthermore, reusing magnetic nanoparticles for wastewater treatment is an environmentally friendly and cost-effective option [86]. However, due to the synthesis method's yield and reproducibility restrictions, the final nanocomposite's stability, and the potential of long-term reuse, this material is not yet often used with its full potential. Furthermore, due to the amorphous form of the precipitates, findings in the literature state that deposition of TiO_2 on SiO_2 coated MNP has a low photocatalytic activity [87].

1.10 Dyes as Industrial Waste

Dyes are special substances that are generally used to protect a surface from external factors or to add color to other colorless substances to increase the attractiveness of the product.

According to Rashid et al. (2020) [88], the textile industry is considered to be one of the largest water consumers, estimated to generate around 100 liters of wastewater for every kilogram of fabric produced. The peculiarity of wastewater produced by the textile industry is that it contains a high concentration of dyes [89]. Even though not many dyes are inherently toxic, wastewater becomes highly resistant to the penetration of sunlight and oxygen into aquatic environments, which are requisite for the survival of aquatic life, in the presence of dyes [90]. One of the most common dyes that have extensive usage in the industry is methylene blue (MB), which is a hazardous dye [91]. MB is an organic dye that belongs to the classes of phenothiazines, aromatic, heterocyclic and it has an alkaline character. Also, it is a water-soluble dye and gives blue-colored cations. Releasing of these organic dyes such as MB is mainly due to textile, paints, palp industry, wood processing [92], silk and cotton industries [93]. Waste MB can lead to instability and eutrophication of aquatic ecosystems by creating a metabolic convulsion in microalgae and reducing oxygenation of water due to inhibition of the photosynthesis because of its toxic level [94]. Additionally, MB is considered biohazardous. Because it is known to be a strong carcinogen for some marine species and causes serious eye irritation,

convulsions, skin sensitivity, and tachycardia in humans [95]. Therefore, ensuring adequate treatment of textile wastes in order to reduce their toxicity and comply with environmental legislation is essential.

1.11 Dye Removal Processes

When a dye removal process is mentioned, the first thing that comes to mind is photocatalyst and especially TiO_2. Researchers have used TiO_2 in many dye removal processes by irradiation of UV, sometimes by itself and sometimes in combination with another dopant. Some applications of TiO_2 in the dye removal processes are given in Table 1.1 below.

Table 1.1 TiO_2 used in the organic dye removal processes by itself or with a dopant from water

Dopant	**Organic Dye**	**Reference**
-	Rhodamine B Congo red Methylene blue	[96]
-	Crystal violet	[97]
Boron (B)	Acid yellow 1	[98]
Carbon (C) Nitrogen (N)	Violet-3B	[99]
Cobalt (Co)	Amido black	[100]
Gold (Au)	Methyl orange	[101]
Gold (Au)	Methylene blue Auramine O Basic red 5 Basic blue 7	[102]
Iron ($Fe3^{+}$) Platinum (Pt^{4+})	Eriochrome black-T	[103]
Iron ($Fe3^{+}$)	Acid orange 7	[104]
Magnesium (Mg)	Congo red	[105]

Also, core-shell-shell structures by including a magnetic core covered with silica, and an outside layer containing a photocatalyst agent, like titanium dioxide have been synthesized to be used in dye removal processes, according to the literature [106-109]. The Fe_3O_4@SiO_2@ZnO:La structure was used by Lv et al. [110] to decompose the methylene blue dye with an efficiency of 81 to 94 percent. Similarly, Fe_3O_4/mesoporous SiO_2/TiO_2, with its mean size of around 450 nm, degrade methyl orange dye with 90 to 95 percent effectiveness in about 120 minutes [111].

CHAPTER 2

2 MATERIALS AND METHODS

2.1 Chemicals and Reagents

Elemental sulfur (Acros Organics, 99.5%), linolenic acid (LNA, Tokyo Chemical Industry), titanium dioxide (TiO_2, Degussa P25), and cobalt ferrite ($CoFe_2O_4$) magnetic nanoparticles (MNP) were used during the preparation of polymer composite materials. Methylene Blue (MB) dye (Sigma Aldrich) was used in photocatalytic applications without being processed.

2.2 Instrumentation

2.2.1 Field Emission Scanning Electron Microscope (FE-SEM)

The morphology and structure of synthesized nanocomposite materials and their components were analyzed using a Quanta 400F Field Emission Scanning Electron Microscope (FE-SEM, METU Central Laboratory).

2.2.2 Transmission Electron Microscopy (TEM)

The morphology and structure of synthesized nanocomposite materials and their components were investigated using 2100 F, 200 kV Transmission Electron Microscopy (TEM, METU Central Laboratory).

2.2.3 Energy Dispersive X-ray Spectrometer (EDX)

The elemental compositions of produced materials were investigated using EDX coupled to a Quanta 400F Field Emission Scanning Electron Microscope (FE-SEM) and a 2100 F, 200 kV TEM.

2.2.4 Fourier Transform Infrared Spectra

Fourier Transform Infrared (FTIR) spectra were obtained using an “Attenuated Total Reflectance” (ATR) unit and a “Thermo Scientific Nicolet” iS10FTIR spectrometer instrument.

2.2.5 Nuclear Magnetic Resonance Spectra

The polymers' nuclear magnetic resonance (NMR) spectra were recorded in d-DMSO or d-$CHCI_3$ using a Bruker DPX-400 Spectrometer. To understand the chemical shifts in ^1H NMR spectra, tetramethylsilane is utilized as an internal standard.

2.2.6 Solar Simulator

ATLAS Solar Simulator the equipped with a metal halide lamp operated at 150 W. used as the light source for the photocatalytic activities of polymeric composites to degrade MB.

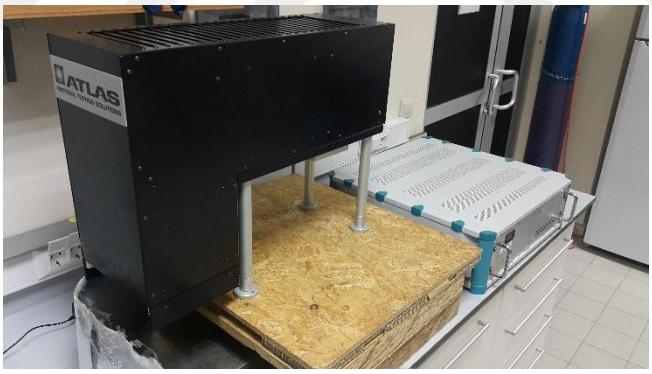

Figure 2.1 ATLAS solar simulator

2.2.7 Centrifugal

Nüve NF 200 bench top centrifuge was used to settle the solids before taking MB sample for UV-Vis Spectrophotometer.

Figure 2.2 Nüve NF 200 bench top centrifuge

2.2.8 Uv-Vis Spectrophotometer

Shimadzu UV-1800 UV-Vis Spectrophotometer was used to figure out the percent degradation of MB dye solution after irradiation.

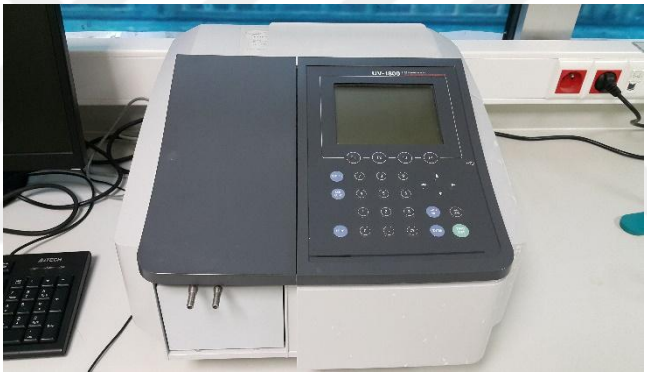

Figure 2.3 Shimadzu UV-1800 UV-Vis Spectrophotometer

2.3 Preparation of Poly(S-r-LnA) Copolymers

Inverse vulcanization method was used to obtain high sulfur content polymers (more than 50 wt%) by just heating sulfur in the presence of fatty acid. In the preparation of polysulfur, linoleic acid (LnA) was used as fatty acid source. Initially different mass percentage of sulfur was tried and 90% sulfur by weight was found as optimum amount. Preparation method is given in Figure 2.4.

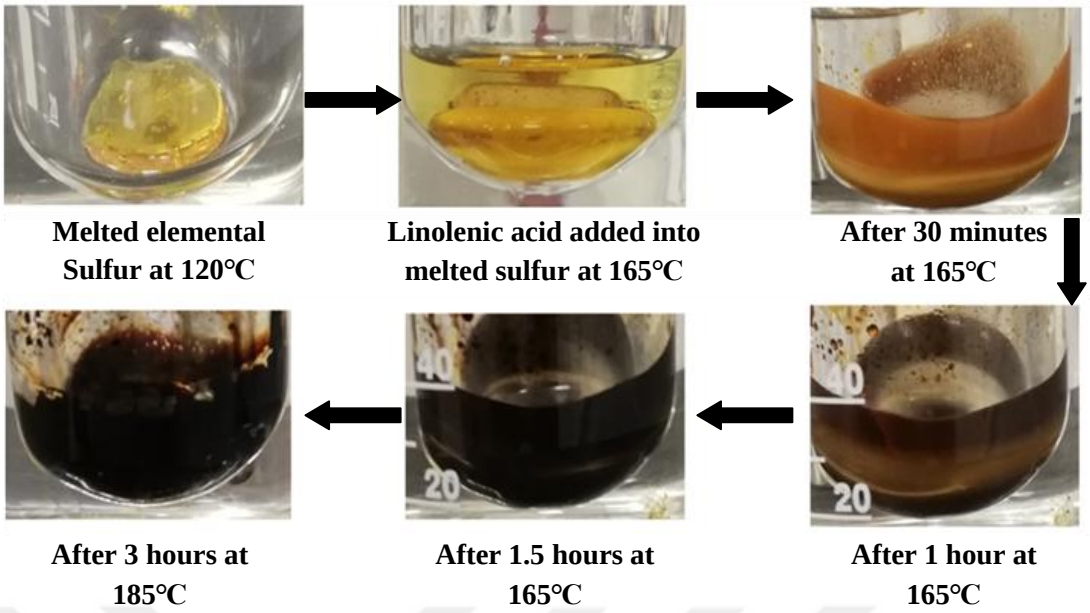

Figure 2.4 Preparation of Poly(S-r-LnA) Copolymer

To prepare 2 g of polysulfur, 1.8 g of sulfur added to test tube and heated up to 165℃. After melting, 0.2 g of LnA was added to molten sulfur and stirred for 1.5 h at 1000 rpm. The temperature was adjusted to 185℃ and controlled with thermocouple. The color of the material turns to black. Finally formed polymer allowed the cool to room temperature and stored for further use.

2.4 Preparation of Poly(S-r-LnA) 90%S- TiO_2-MNP Composite Material

In the synthesis of polymeric composites containing TiO_2 and MNP, they were put into the test tube together with sulfur at the beginning of the heating process and blended to get a homogeneous mixture, and the same process is followed to synthesize polysulfide copolymers.

Figure 2.5 Sulfur, titanium dioxide, and magnetic nanoparticles mixture in a test tube (Yellow powder sulfur, white powder is TiO_2, black powder MNP)

The specified mass of elemental sulfur and fatty acid is determined according to the percentages by weight (e.g. for 2.0 g of polymer with 90% sulfur and 10% fatty acid; 1.8 g sulfur and 0.2 g fatty acid). Elemental sulfur was weighed on a balance and put into a test tube. For the polymers which include TiO_2 and $CoFe_2O_4$ MNP, these materials were added to the polymers at this step and each one was added up to 1/5 of the total weight of the polymer (e.g. for 2.0 g of polymer; 0.4 g of TiO_2, and 0.4 g of MNP). Then the test tube was heated until 165℃ by using a thermocouple while half-length submerged in heating oil and also when the mixture was liquefied (at around 120℃, the sulfur rings, which form the main chain of the polymer, open and liquefy) it was stirred at around 1000 rpm by using a magnetic stirrer to have a homogeneous mixture (the mixture which has TiO_2 during heating would not be liquefied and cannot be mixed until fatty acids are added). After that, the desired amount of oleic acid, which is in the liquid state, was dropped into the test tube and waited around 1-1.5 hours. During the heating process, the color of the mixture changed from yellow to dark brown and kept that color after polymerized (for the polysulfide that contains MNP, the color turns black as shown in Figure 2.5). Then, the temperature was set to 185℃ and heated for around 1-1.5 hours more. At the end of this time, heating and stirring were stopped but the test tube is waited inside the heating oil to cool slowly. Finally, the size of the copolymer was reduced by using a mortar and stored in an Eppendorf tube.

Figure 2.6 Powdered polysulfide copolymer (on the left) and polysulfide composite material with TiO_2 and MNP (on the right)

2.5 Photocatalytic Applications

Photocatalytic activity of all materials was tested by using the ATLAS solar simulator as a light source. Methylene blue dye was chosen as a model compound for textile-based wastewater. (Figure 2.6). For photocatalytic degradation of MB under solar light, 20 mg of catalyst in the powder was dispersed in 10 mL of MB solution which is 2.0×10^{-5} M. Then 500 μL of ethanol was added to the mixture to reduce the surface tension and increase the dispersion of copolymer in the MB solution. After that mixture was irradiated for 10, 30, 60, and 120 minutes. At each time 2 mL portion of the mixture was isolated by centrifugation and degradation of MB was followed with UV-Vis measurements by using the Shimadzu UV-1800 UV-Vis Spectrophotometer. For the composite material, the catalyst was separated by using an external magnet.

Figure 2.7 Dye removal process of polysulfide materials under solar simulator

Finally, the percent value of the MB degradation was calculated by using the following formula. % Removal of MB dye = A MB stock solution – A light treated sample/A MB stock solution × 100 (A: absorbance value) For reuse studies, the photocatalyst was isolated by using an external magnet then washed, and used for the next cycle of catalytic reaction with a fresh MB solution

CHAPTER 3

3 RESULTS AND DISCUSSION

In this thesis, polysulfide copolymers (poly(S-r-LnA)) were prepared by inverse vulcanization method and used as support material for the preparation of semiconductor, TiO_2 nanoparticle, based photocatalytic material with a magnetic property. Initially, poly(S-r-LnA) copolymer was prepared. In this part, different mass ratios of sulfur and LnA was tried and poly(S-r-LnA)-90wt% S (90%S-10%LnA) was found as proper structure as support material. After that, TiO_2 nanoparticles and magnetic nanoparticles were added to poly(S-r-LnA)-90wt% S support material, and poly(S-r-LnA)-TiO_2-MNP composite material was produced. The characterization of the copolymer, composite material, and their components was performed by using SEM, TEM, EDX, FTIR, and NMR. Then, the photocatalytic activity of poly(S-r-LnA)-TiO_2-MNP composite material was investigated in the degradation of MB dye under solar light. Also, the photocatalytic activities of the poly(S-r-LnA)-90wt% S and TiO_2 nanoparticles were investigated to make a comparison. Finally, the stability of the poly(S-r-LnA)-TiO_2-MNP composite material was investigated by repeating the dye degradation procedure five times.

3.1 Characterization of the Prepared Materials

Initially, the formation of poly(S-r-LnA) copolymer was proven by using FTIR and NMR spectroscopy. Results are given in Figures 3.1, 3.2 and 3.3 respectively.

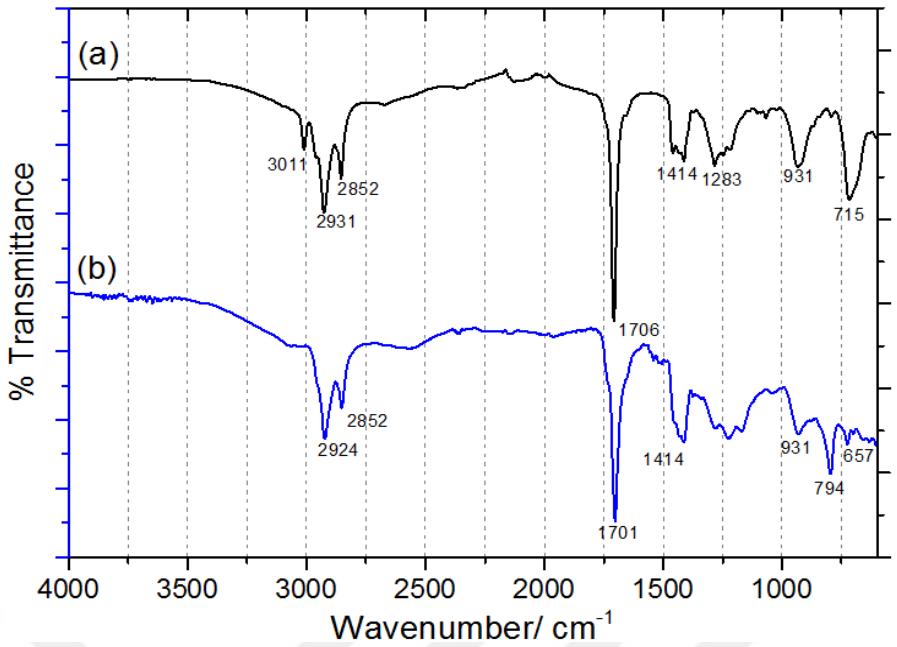

Figure 3.1 FTIR spectra analysis of a) LnA (black curve), b) poly(S-r-LnA) copolymer (blue curve)

The peak located at around 3011 cm^{-1} is referring to the stretching of C-H molecules in the fatty acid and 715 cm^{-1} (C-H out of plane bending mode) is imputed to the double bond and that peak is disappeared after carbons bond with sulfurs. So that the peak at 657 cm^{-1}, which is referring to C-S bond stretching, is formed on the blue curve. There is a very strong C=O peak around 1706 cm^{-1} which is not disappeared after polymerization that means it still has a carboxyl group.

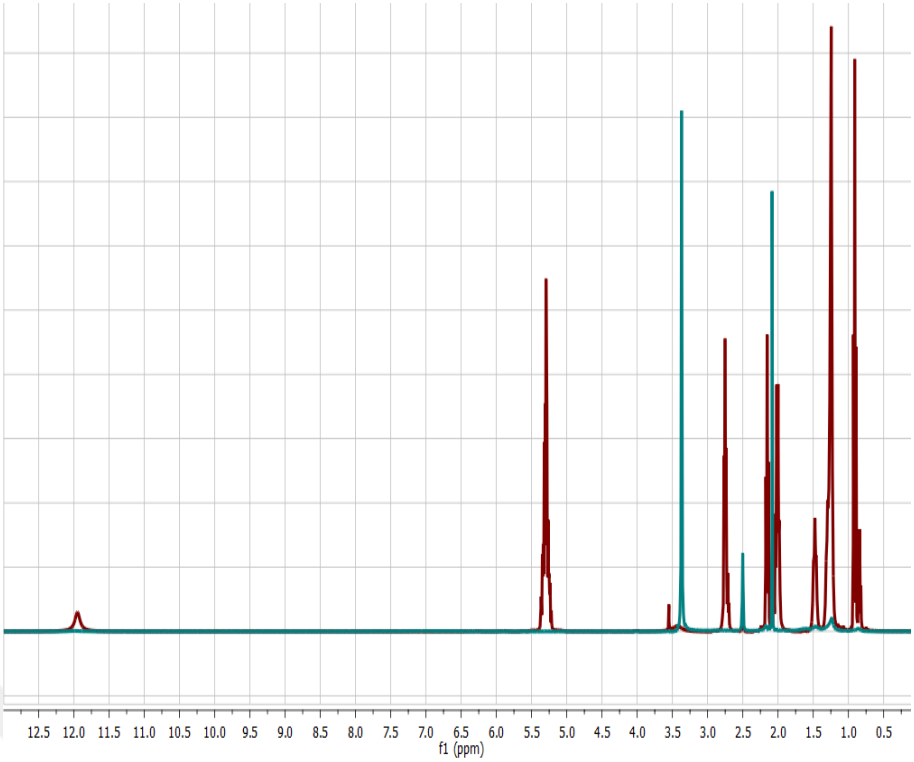

Figure 3.2 ^{1}H NMR spectra of LnA (red) d-DMSO and poly(S-*r*-LnA) copolymer in d-$CHCl_3$

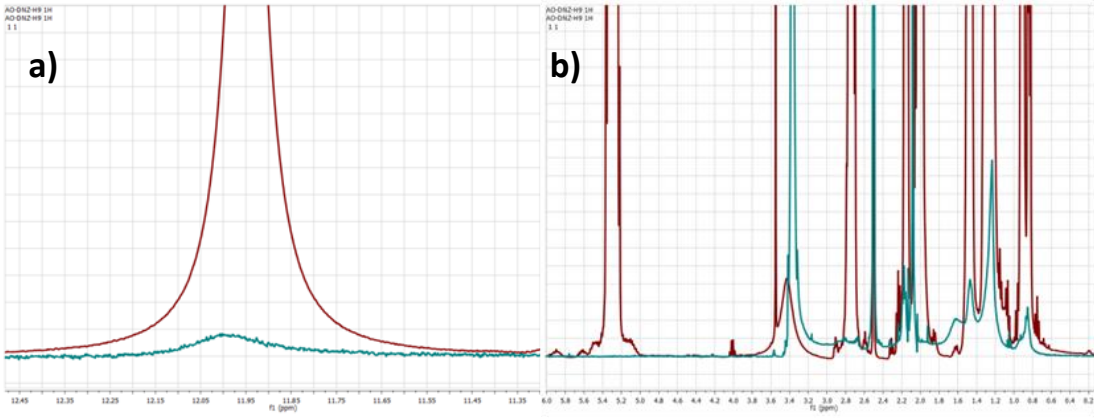

Figure 3.3 ^{1}H NMR spectra of LnA (red) in d-DMSO and poly(S-r-LnA)- 90 wt% S copolymer in d-CHCl3, (A) between 11.35 and 12.45 ppm and (B) between 0.6 and 6.0 ppm

In the spectrum of poly(S-r-FA), the signal of the protons (5.32 ppm) assigned to the double bonds vanished completely (Figures 3.2 and Figure 3.3). Also, the wide signal centered at 12.00 ppm are the protons of carboxylic acid groups. In addition,

between 2.5 and 3.6 ppm, the creation of -S-CH- groups can be seen as a new signal group.

SEM measurements were also performed to determine the morphology of the poly(S-r-LnA) copolymer. Energy-dispersive X-ray (EDX) spectroscopy was used that is coupled with SEM to study the chemical composition of the copolymer. Results are given in Figure 3.4 and Figure 3.5 respectively.

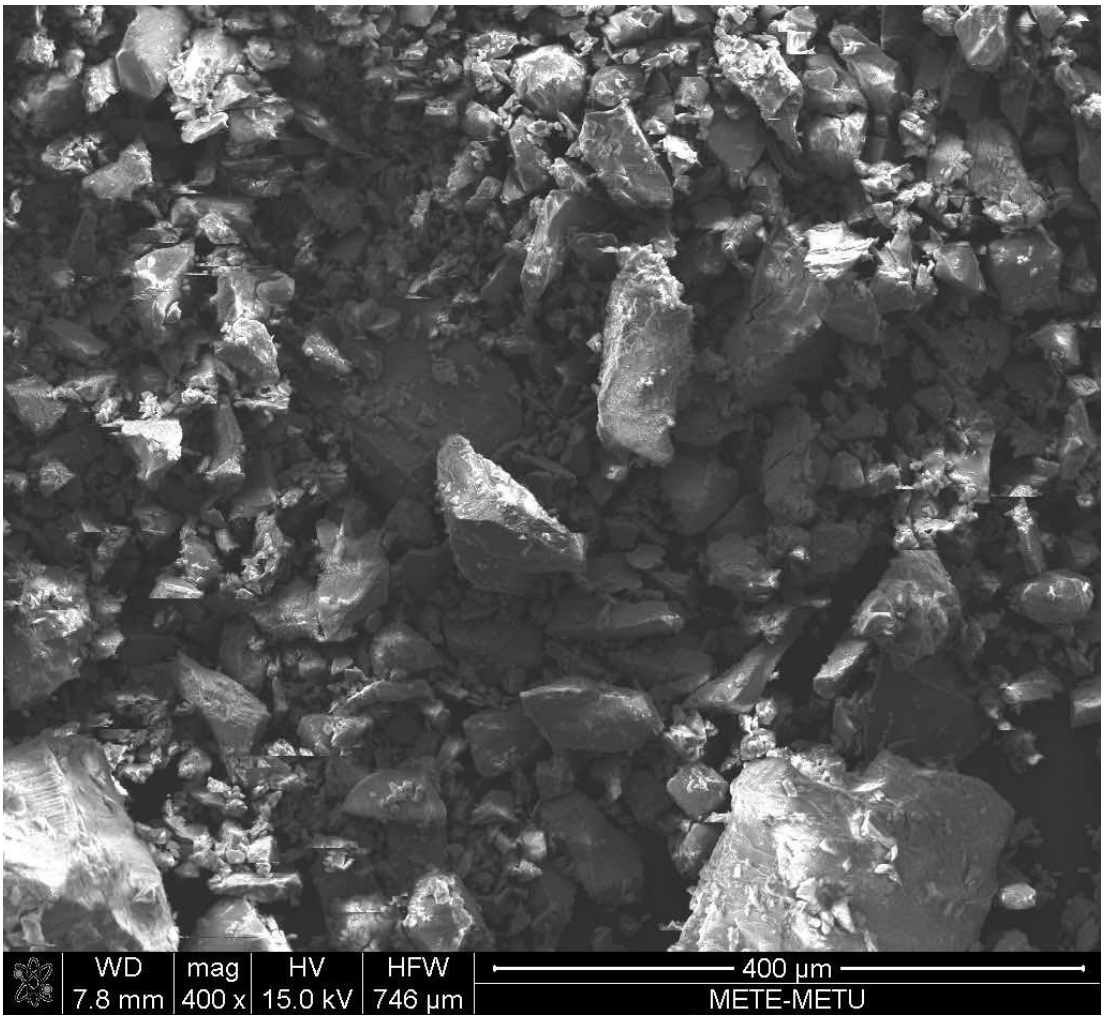

Figure 3.4 SEM image of poly(S-r-LnA)90%S copolymer

As can be observed in the SEM image, a non-uniform size distribution with micron-sized particles has been formed. The chemical composition of the polymeric material was then evaluated using the EDX measurement (Figure 3.5).

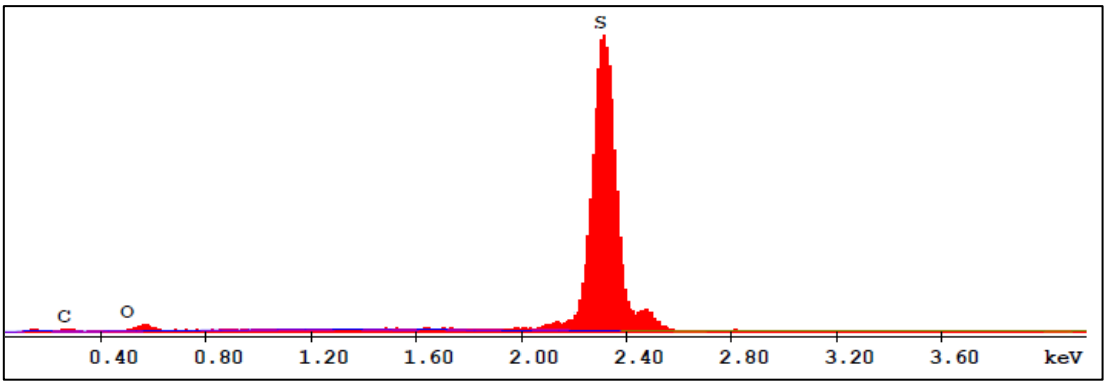

Figure 3.5 EDX pattern of poly(S-r-LnA) 90%S copolymer

As can be seen from Figure 3.5, poly(S-r-LnA) 90%S copolymer contains only S, C, and O.

After the preparation of poly(S-r-LnA) 90%S copolymer, poly(S-r-LnA) 90%S-MNP-TiO_2 composite material was produced by applying the same procedure in the presence of magnetic nanoparticles and TiO_2 nanoparticles. The morphological characterization of poly(S-r-LnA) 90%S-TiO_2-MNP composite material and their components (magnetic nanoparticles and TiO_2 nanoparticles) was carried out by using TEM, SEM, and EDX measurements. Results are given below.

Initially, TEM measurement of TiO_2 nanoparticles was performed. The result is given in Figure 3.6.

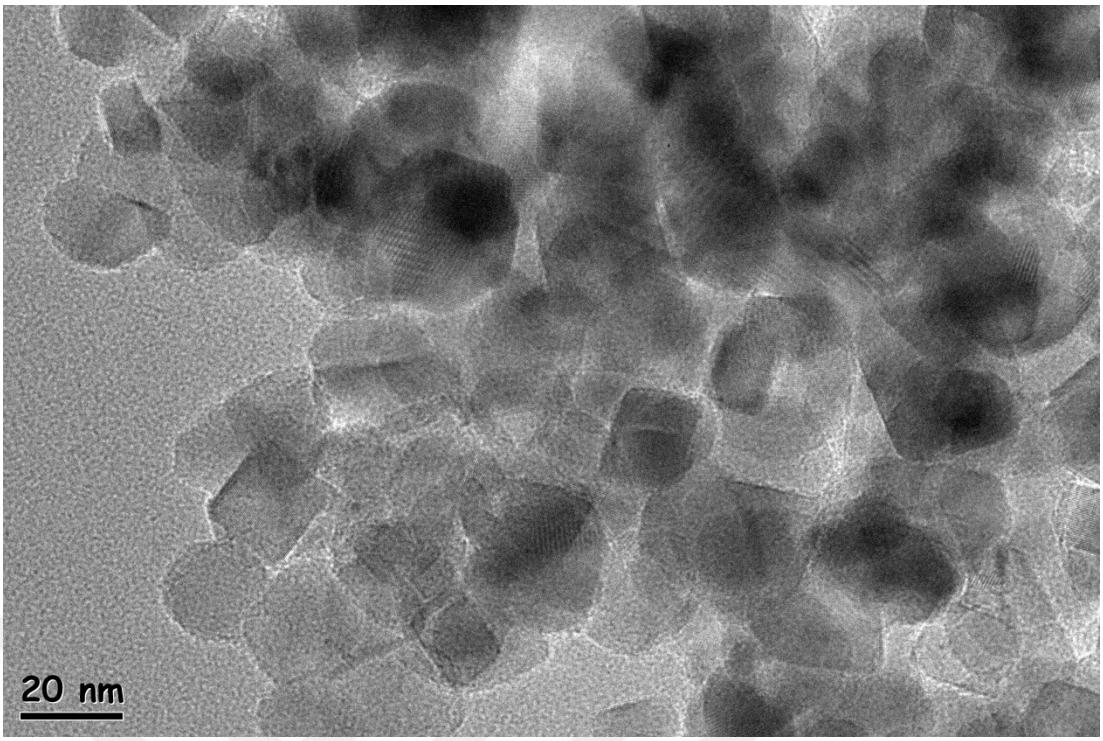

Figure 3.6 TEM image of the TiO_2 nanoparticles (Degussa P25)

Nearly 50 particles were randomly selected from the TEM picture in Figure 3.6, and the particle size of TiO_2 nanoparticles was calculated as 25±5 nm.

After that TEM measurement of magnetic nanoparticles (cobalt ferrite, $CoFe_2O_4@SiO_2$) was performed to reveal their size. TEM image is given in Figure 3.7.

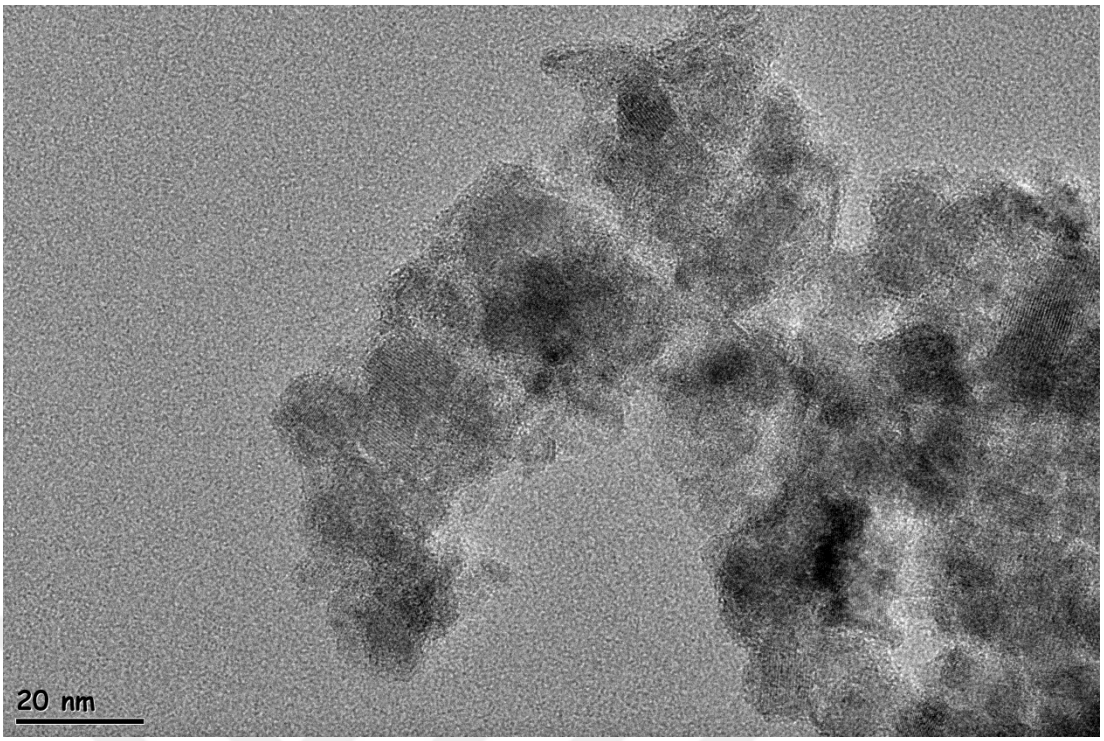

Figure 3.7 Silica-coated MNP's TEM image.

The size of the magnetic nanoparticles was calculated as 15±2 nm from the image shown in Figure3.7.

Finally, SEM and EDX measurements of poly(S-r-LnA)-TiO_2-MNP composite material were performed to see the change in the morphology and prove the addition of magnetic nanoparticles and TiO_2 nanoparticles. Results are given in Figure 3.8 and Figure 3.9 respectively.

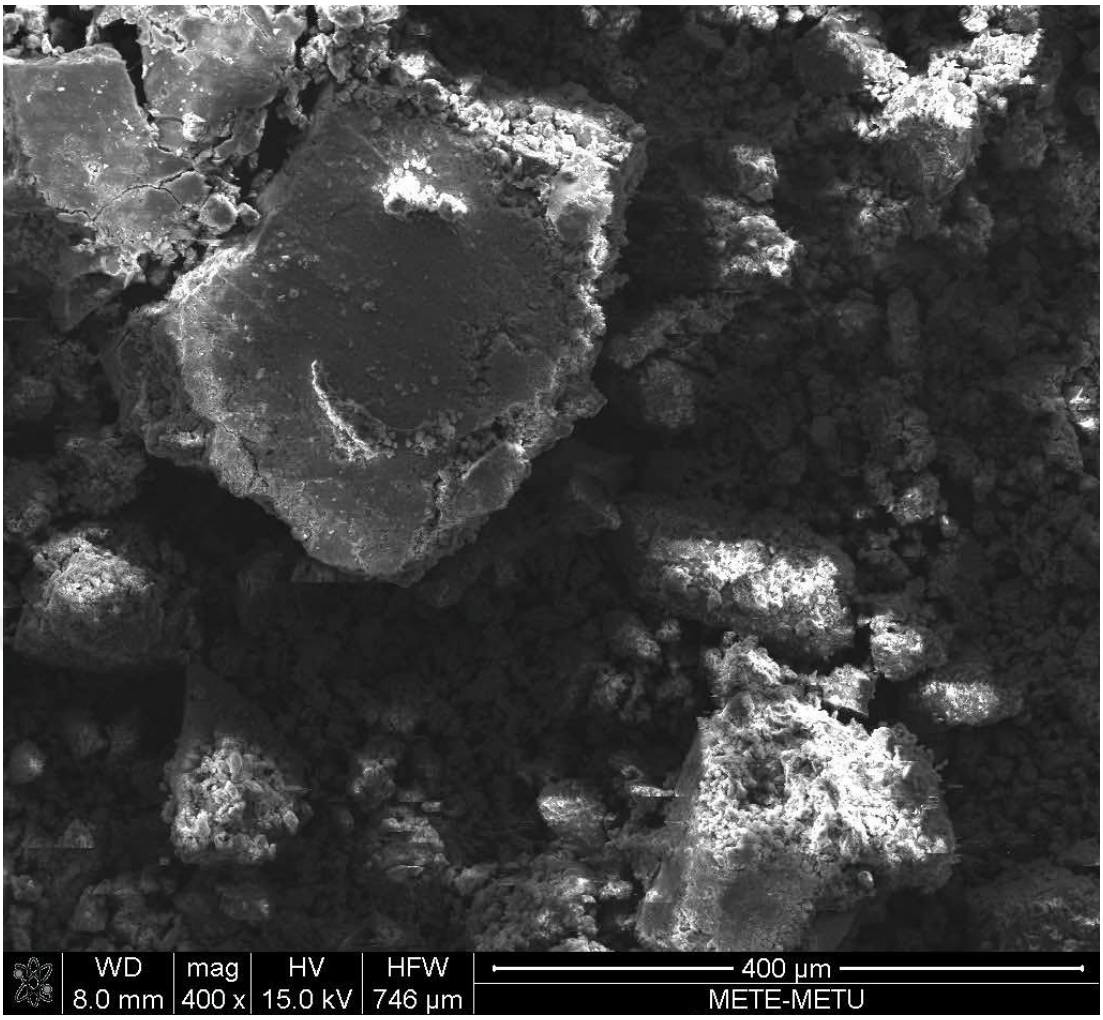

Figure 3.8 SEM image of poly(S-r-LnA)-TiO_2-MNP

According to the SEM image of poly(S-r-LnA)-TiO_2-MNP composite material, it can be said that titanium nanoparticles are attached to the surface of the poly(S-r-LnA) copolymer

The chemical composition of the resulting material was investigated with EDX measurement. The result is given in Figure 3.9.

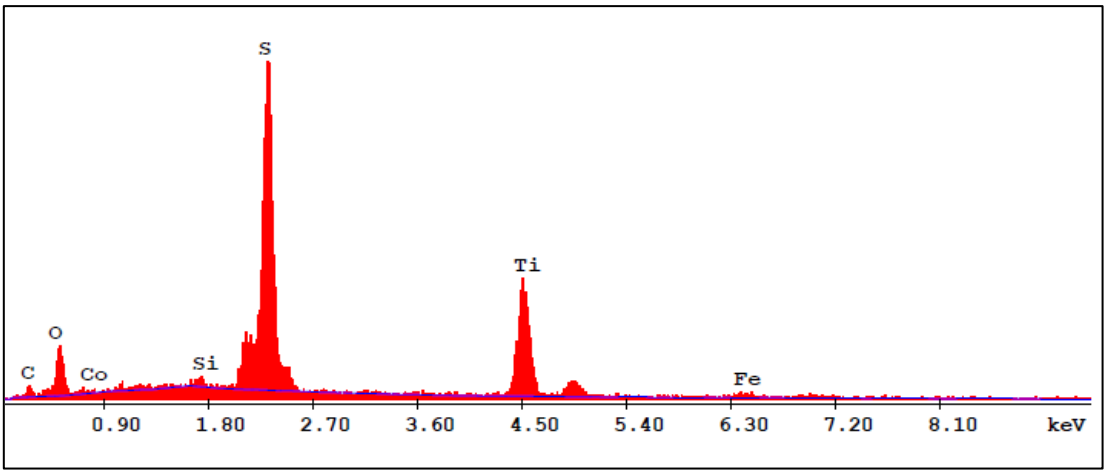

Figure 3.9 EDX pattern of poly(S-r-FA)-TiO_2-MNP

EDX pattern of poly(S-r-FA)-TiO_2-MNP proves the addition of magnetic nanoparticles and titanium dioxide nanoparticles to composite materials.

3.2 Photocatalytic Performance of the Prepared Polymers

To evaluate the photocatalytic activities of prepared nanocatalysts, MB was chosen as a model compound. As it is known, the bright blue color of the MB aqueous solution is due to its light absorption around 665 nm.

The photocatalytic degradation of the MB solution driven by a proper catalyst causes a smooth decrease in the absorption peak. Finally, when the degradation of the dye is completed, the solution becomes colorless.

In dye removal experiments, first of all, to see the photocatalytic effects of the copolymer, the UV-Vis spectrum and percent removal values obtained from the polymers that do not contain titanium dioxide and magnetic nanoparticles with the percentage of 90 of sulfur by weight were examined in the dark environment to be able to determine the absorption-desorption behaviors (Figure 3.10). The amount of dye adsorbed by the polymer was determined to make a comparison. In addition, the self-degradation of MB under a solar simulator in the absence of the polymer was studied to make a comparison.

Figure 3.10 Dark environment dye removal was carried out by covering the beaker with aluminum foil

After dark environment results were obtained, dye removal processes were started with the help of a solar simulator. Among these polymers, the most effective ones were chosen for each fatty acid content copolymer, and the production of polymeric composites containing TiO_2, and $CoFe_2O_4$ MNP at the same percentages of sulfur was carried out. Finally, the dye removal percentages of the copolymers with the same sulfur amount containing TiO_2 and MNP were found. The reference curve is taken from the UV-Vis spectrum by using MB solution at 1 absorbance with the base line of distilled water.

3.2.1 Dark Measurements of Poly(S-r-LnA)-90wt% S Copolymers

Inıtially adsorption behavior of 3 composite materials (Poly(S-r-LnA)-90wt% S) was investigated. For this, 20 mg of the copolymer was mixed in 10 mL of methylene blue in the dark environment. Experiments started with the adsorption behavior of Poly(S-r-LnA)-90wt% S copolymer. UV –Vis spectra and percent degradations are given in Figure 3.11 and Table 3.1.

According to the results, at the end of the 120 minutes stirring under dark 17 % reduction in MB concentration was obtained with the usage of poly(S-r-LnA)-90wt% S copolymer.

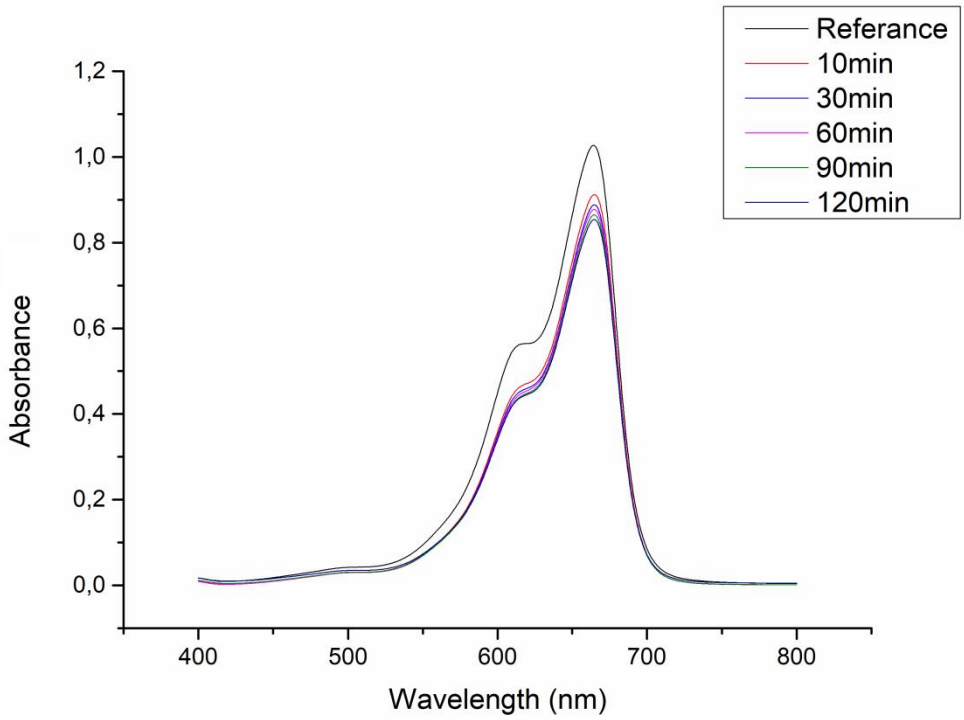

Figure 3.11 Dark measurement of poly(S-r-LnA)-90wt% S copolymer

Table 3.1 The decrease in absorbance of MB treated with Poly(S-r-LnA)-90wt% S copolymer under the dark condition at different time durations.

Time (min)	**Dye Removal (%)**
10	11
30	14
60	15
90	16
120	17

Therefore, it was observed that the adsorption equilibrium was almost achieved with a 10-minute mixing before exposing the mixture containing the catalyst and methylene blue to a solar simulator.

3.2.2 Methylene Blue Self-Degradation Under Solar Simulator

The percentage of self-degradation of the dye was determined by directly exposing 10 mL of methylene blue at 1 absorbance to the solar simulator in a polymer-free environment.

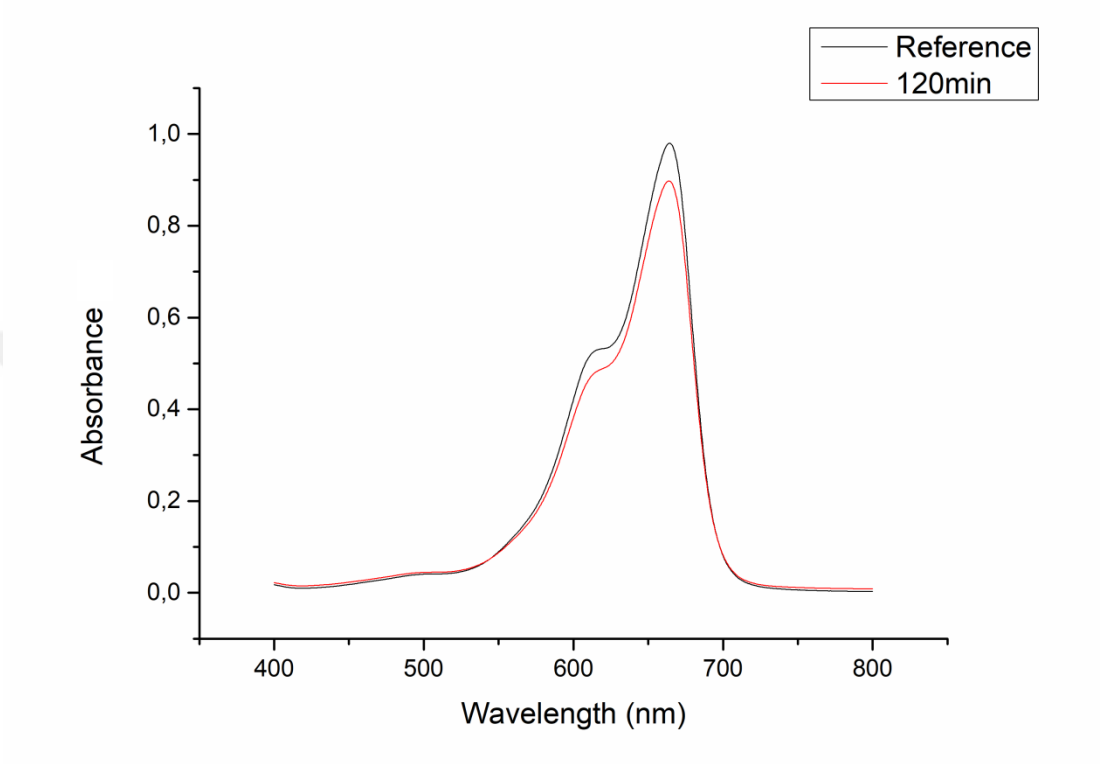

Figure 3.12 Self-degradation profile of methylene blue under solar simulator

Accordingly, a 9% self-degradation was detected in the methylene blue solution exposed to solar light at the end of the 120 minutes.

After investigating the adsorption behavior of poly(S-r-LnA)-90wt% S copolymers, the photocatalytic activity of the copolymer with 90% sulfur content by weighing and the composite materials prepared with the addition of magnetic and titanium nanoparticles were investigated in the MB degradation under solar light. In all photocatalytic measurements, 20 mg photocatalytic material was mixed with 2.0×10^{-5} M MB solution (1A) and exposed to solar light under stirring conditions. After a certain time, a 2 mL portion of the MB solution was taken from the reaction mixture. After isolation of the solid catalyst, UV-Vis measurement was performed, and

percent degradation was calculated by following the absorption peak located at 665 nm. After that, a 2 mL portion was added to the initial mixture, and light exposure was continued. This process was repeated until the end of the photocatalytic process. After following the decrease in absorption maxima, the percent removal of MB was calculated by using the equation given in the experimental part. In all measurements, a blank correction was applied. The ± standard deviation of all UV-Vis measurements performed was calculated around 1 % during this study.

3.2.3 Photocatalytic Dye Removal of Poly(S-r-LnA)-90wt% S Copolymer

The photocatalytic activity of the poly(S-r-LnA)-90wt% S was investigated in the MB degradation under solar light exposure. MB absorption maxima were measured at a specific time, and the change in dye concentration was followed by a UV-Vis spectrophotometer. Results are given in Figure 3.13 and Table 3.2.

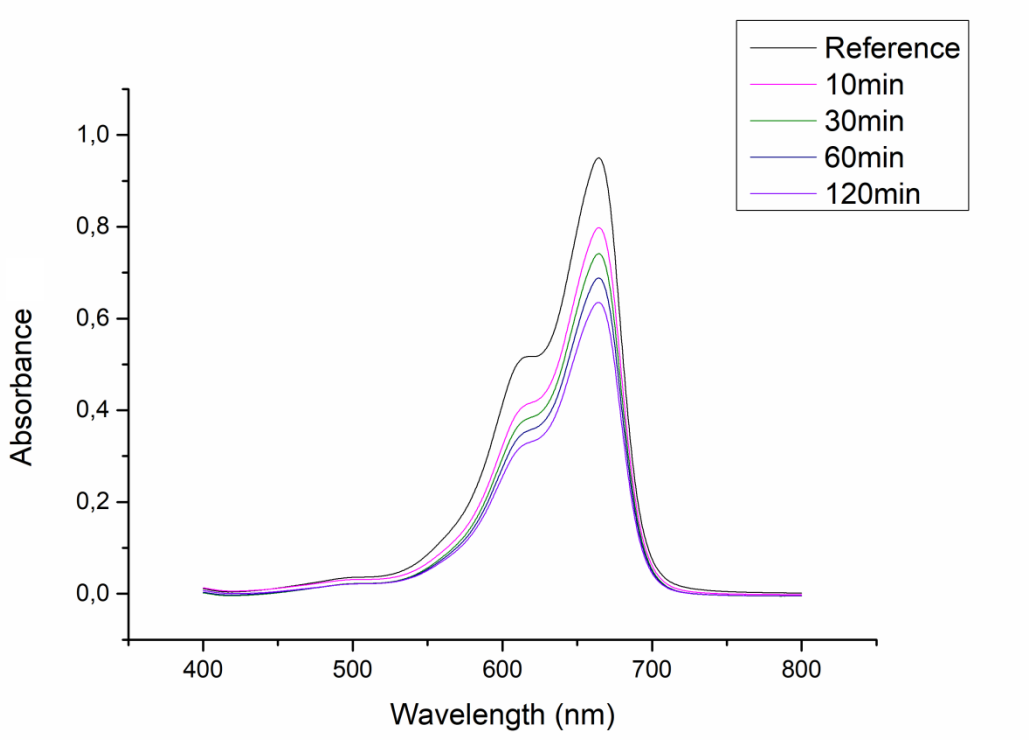

Figure 3.13 UV-Vis spectra of the MB solution after treatment with poly(S-r-LnA)-90wt% S copolymer under solar light

Table 3.2 The percent dye removal obtained with the use of poly(S-r-LnA)-90wt% S copolymer

Time (min)	**Dye Removal (%)**
10	16
30	21
60	27
120	33

As seen from the result after 120-minute exposure to solar light only 33% of the MB was degraded.

In the following sections, the most effective polymers which have 90% sulfur and 10% fatty acid content by weight were resynthesized using TiO_2 and MNP and exposed to the solar simulator for 120 minutes for the dye removal processes.

3.2.4 Photocatalytic Dye Removal of Poly(S-r-LnA)-90wt% S Polymeric Composite Including Titanium Dioxide and Magnetic Nanoparticles

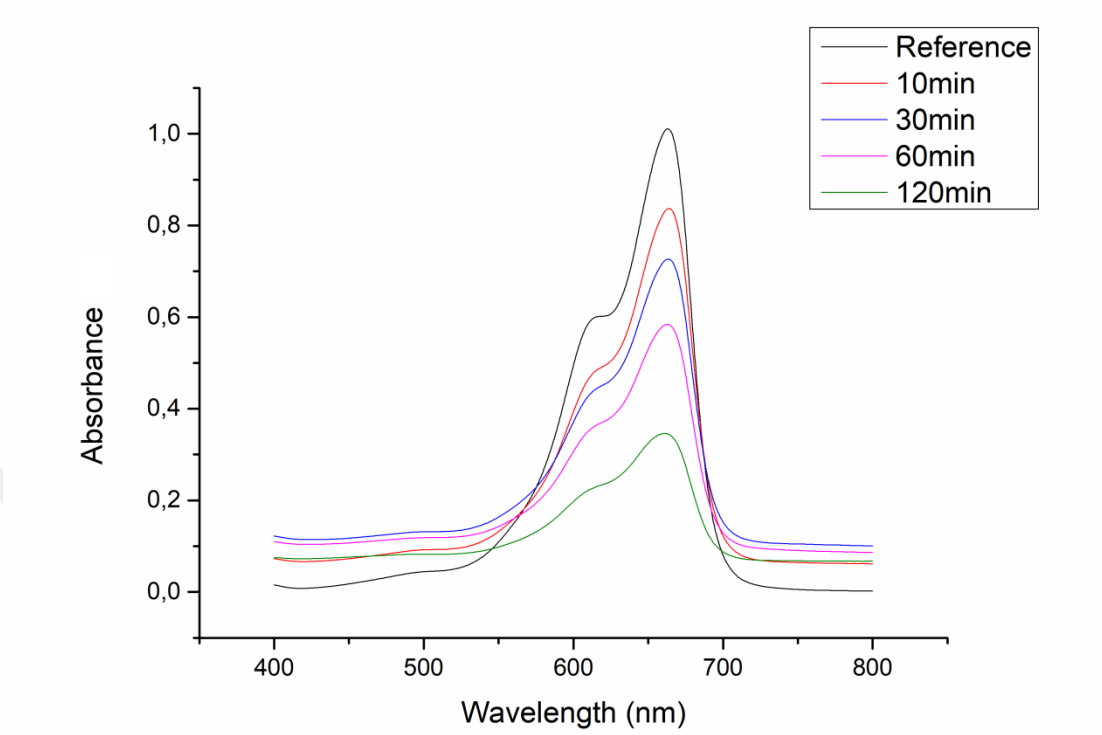

Figure 3.14 UV-Vis spectra which show the photocatalytic degradation of MB by using 20 mg poly(S-r-LnA)-90wt% S-TiO_2-MNP polymeric composite material under solar light

Table 3.3 Poly The percent dye removal obtained with the use of poly(S-r-LnA)-90wt% S-TiO_2-MNP composite material

Time (min)	Dye Removal (%)
10	23
30	38
60	51
120	73

In the results given above, at the end of 120 minutes, 73% removal was obtained with the use of poly(S-r-LnA)-90wt% S-TiO_2-MNP composite material. The catalytic activity of poly(S-r-LnA)-90wt% S increases from 33% to 73 % with the addition of 4 mg TiO_2 nanoparticles.

To show the importance of the poly(S-r-LnA)-90wt% S copolymer as a support material, the catalytic activity of pure TiO_2 nanoparticles was also investigated in the same reaction under the same conditions. The obtained result was used as a reference for comparison to figure out the catalytic performance of the novel poly(S-r-LnA)-90wt% S-TiO_2-MNP composite materials prepared during this study. Results are given in Figure 3.15 and Table 3.4.

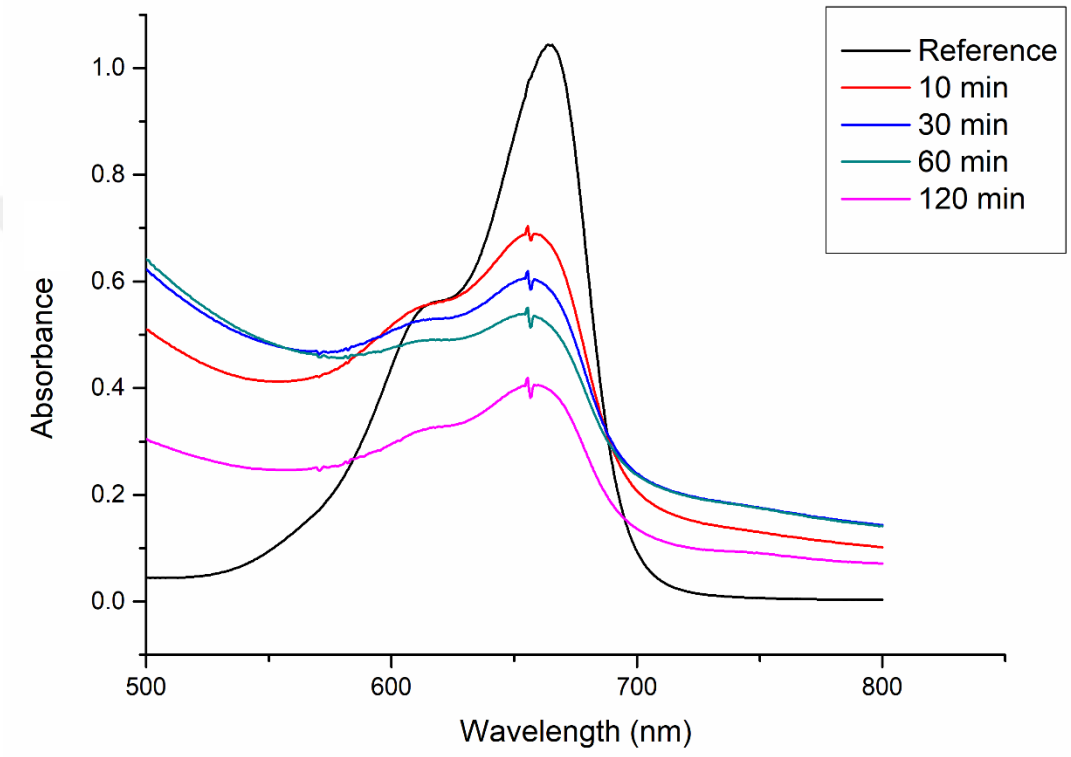

Figure 3.15 UV-Vis spectra of MB photocatalytic degradation by using 20 mg TiO_2 nanoparticles (Degussa P25) as a photocatalyst under solar light.

Table 3.4 The percent dye removal obtained with the use of 20 mg TiO_2 nanoparticles (Degussa P25) as a photocatalyst

Time (min)	**Dye Removal (%)**
10	30
30	39
60	50
120	65

The comparison of the percent degradation of poly(S-r-LnA)-90wt%, poly(S-r-LnA)-90wt% S-TiO_2-MNP composite material, and TiO_2 nanoparticles is given in Figure 3.16.

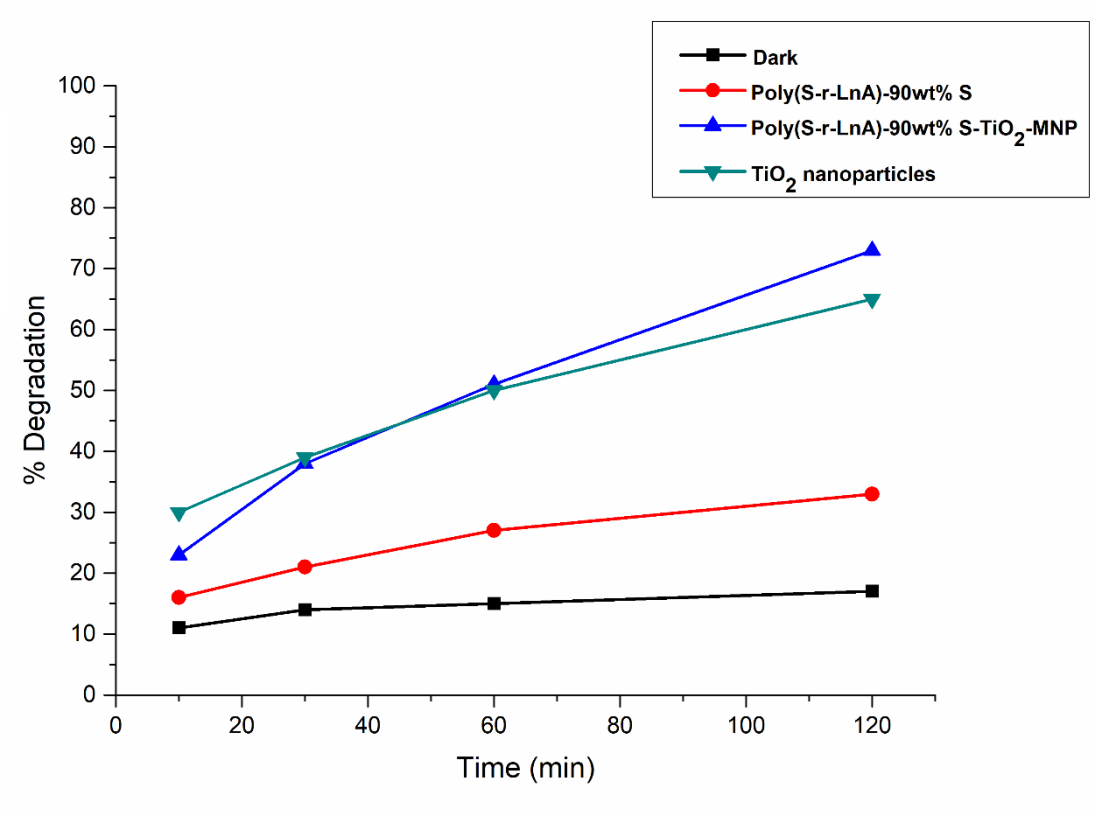

Figure 3.16 Comparison of the catalytic activities of the poly(S-r-LnA)-90wt%S, poly(S-r-LnA)-90wt% S-TiO_2-MNP composite material, and TiO_2 nanoparticles used for MB degradation under solar light.

From the results given above, 65 % degradation of MB was achieved by TiO_2 nanoparticles after 120-minute exposure to solar light. In the case of poly(S-r-LnA)-90wt%S, 33 % degradation of MB was achieved under the same conditions. With the usage of composite material poly(S-r-LnA)-90wt% S-TiO_2-MNP, obtained with the addition of TiO_2 and magnetic nanoparticles, 73% degradation of MB under solar light was achieved. As can be seen from the results, the highest photocatalytic activity was observed with the usage of poly(S-r-LnA)-90wt% S-TiO_2-MNP composite material.

Considering that only 14% of the poly(S-r-LnA)-90wt% S-TiO_2-MNP composite material is titanium nanoparticle (20 mg composite material contains 2.8 mg TiO_2

nanoparticles), the catalytic activity of composite material is higher than that of the 20 mg TiO_2 nanoparticles. This can be attributed to the dispersion of TiO_2 nanoparticles on the surface of the copolymer besides the increase in surface roughness and porosity.

3.3 Stability of Poly(S-r-FA)-TiO_2-MNP Composite Material as Photocatalyst

Another advantage of the poly(S-r-LnA)-TiO_2-MNP composite material besides the high photocatalytic activity can be considered as magnetic separation. Due to the magnetic property added to the composite material, it can be isolated easily from the reaction medium with the help of an external magnet in a short time without the need for separation processes that require a long time. So it is possible to use the same catalyst in other cycles and also the pollution caused by the catalyst is prevented. This advantage is achieved through the poly(S-r-LnA) copolymer because it keeps titanium and magnetic particles together in the poly(S-r-LnA)-TiO_2-MNP composite material while increasing the dispersion of TiO_2 nanoparticles at the surface.

The reuse performance of poly(S-r-LnA)-TiO_2-MNP composite material was investigated by performing five successive tests in the degradation of MB under solar light. After the first run of photocatalytic degradation of MB performed under solar light, poly(S-r-LnA)-TiO_2-MNP composite material was isolated magnetically from the reaction mixture.

The separated particles were then dispersed in a fresh 10 mL MB solution. Then, for the next 120 minutes, solar light irradiation was initiated. Using the same catalyst, this process was performed five times in total. The result for each run is given in Figure 3.17.

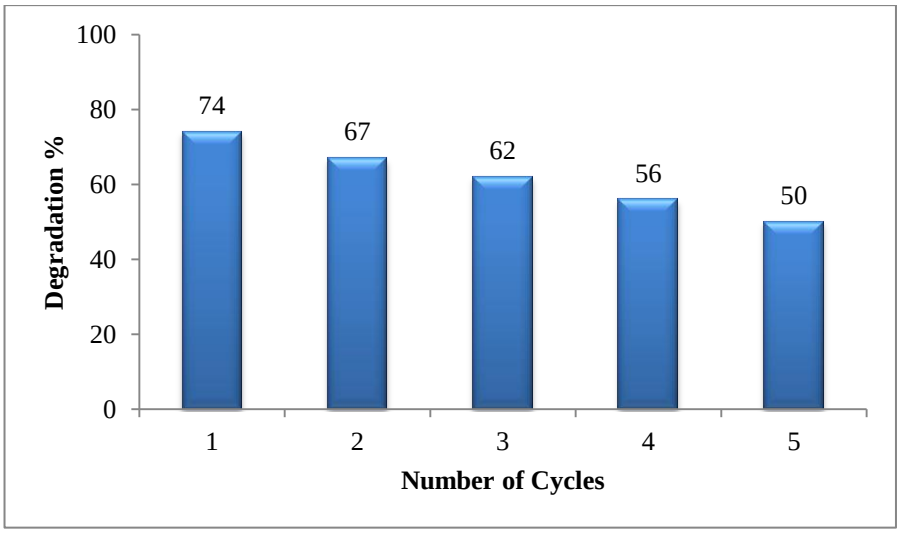

Figure 3.17 Reuse capacity of the Poly(S-r-LnA)-TiO_2-MNP composite material as photocatalyst in the degradation of MB

The percent degradation value, which indicates the catalytic activity of the poly(S-r-LnA)-TiO_2-MNP composite material, decreased about 24% after five trials. Although the percentage degradation value decreases slightly, the particles may be easily extracted from the reaction mixture without the need for time-consuming procedures like centrifugation or filtration, and without producing secondary pollution.

According to the results given above, it can be concluded that poly(S-r-LnA)-TiO_2-MNP composite material has high stability as a photocatalyst. The slight decrease in photocatalytic activity can be attributed to the loss of catalyst during separation from the reaction mixture and deposition of degradation products onto the composite material.

CHAPTER 4

4 CONCLUSION

In environmental remediation, semiconductor materials are frequently utilized in photocatalytic reactions. Titanium dioxide nanoparticles are the most extensively used semiconductor. These particles, on the other hand, only exhibit high catalytic activity when exposed to UV light and the entire cost of environmental remediation rises as a result of this. As a consequence of that, studies on the development of photocatalytic materials in which reduces the usage of semiconductors and can work under solar light are becoming increasingly important in order to minimize the total cost of the process. To minimize the operation cost and prevent the pollution caused by the catalyst, isolation, and reuse of the photocatalyst are also important points.

In this study, polysulfide copolymer, poly(S-r-LnA) were synthesized by elemental sulfur and renewable diene monomers, fatty acid (linolenic acid), with different mass ratios, via inverse vulcanization. After that, the prepared copolymer was used as a support, material for the preparation of photocatalytic material to perform the degradation of model dye MB, simulant for textile-based wastewater, under solar light. For this semiconductor TiO_2 nanoparticles were added to the structure. Also to increase the stability and reuse performance of the photocatalytic material cobalt ferrite magnetic nanoparticles were added to the structure. After preparation, the detailed characterization of poly(S-r-LnA)-TiO_2-MNP composite material and their components was performed by using SEM, TEM, EDX, FTIR, and NMR. Then the photocatalytic activity of poly(S-r-LnA)-TiO_2-MNP composite material and their components was investigated.

According to the results, the catalytic activity of pure TiO_2 nanoparticles was increased when placed on support material, poly(S-r-LnA) copolymer. Higher activity was achieved despite using much fewer titanium nanoparticles. Besides

poly(S-r-LnA) copolymer allows the addition of MNP to the structure which gives the easy separation property to the final composite material.

With this property, poly(S-r-LnA)-TiO_2-MNP composite material easily recovered by using an external magnet and used for the next cycle. For this reason, poly(S-r-LnA) copolymer can be considered as a good support material for the preparation of semiconductor-based photocatalysts.

REFENRENCES

[1] R. Steudel, "Liquid Sulfur," in *Elemental Sulfur and Sulfur-Rich Compounds I, ,* vol. 230, Berlin: Topics in Current Chemistry, 2003, pp. 81-116.

[2] R. F. Bacon and R. Fanelli, "The Viscosity of Sulfur1," *Journal of the American Chemical Society,* vol. 65, no. 4, pp. 639-648, April 1 1943.

[3] M. J. H. Worthington, R. L. Kucera, and J. M. Chalker, "Green chemistry and polymers made from sulfur," *Green Chemistry,* vol. 19, no. 12, pp. 2748-2761, 2017.

[4] J. J. Griebel, R. S. Glass, K. Char, and J. Pyun, "Polymerizations with elemental sulfur: A novel route to high sulfur content polymers for sustainability, energy and defense," *Progress in Polymer Science,* vol. 58, pp. 90-125, 2016.

[5] "L. A. Apadoca, “Mineral Commodity Summaries 2020”. U.S. Geological Survey, pp. 161-162, 2020.."

[6] G. Kutney, "Le Rui De Sol," in *Sulfur History, Technology, Applications & Industry,* 2nd ed. Toronto: ChemTec Publishing, September 30, 2013, pp. 1-4.

[7] J. A. Ober. "Materials Flow of Sulfur, Open-File Report 02–298, U.S. Department of the Interior, U.S. Geological Survey", Internet: https://pubs.usgs.gov/of/2002/of02-298/ 2003 [December 23,2021].

[8] J. Lim, J. Pyun, and K. Char, "Recent approaches for the direct use of elemental sulfur in the synthesis and processing of advanced materials," *Angew Chem Int Ed Engl,* vol. 54, no. 11, pp. 3249-58, Mar 9 2015.

[9] W. J. Chung *et al.,* "The use of elemental sulfur as an alternative feedstock for polymeric materials," *Nat Chem,* vol. 5, no. 6, pp. 518-24, Jun 2013.

[10] J. A. Smith, X. Wu, N. G. Berry, and T. Hasell, "High sulfur content polymers: The effect of crosslinker structure on inverse vulcanization," *J Polym Sci A Polym Chem,* vol. 56, no. 16, pp. 1777-1781, Aug 15 2018.

[11] Q. Adam, R. Behnke, and M. Kaliske, "A thermo-mechanical finite element material model for the rubber forming and vulcanization process: From unvulcanized to vulcanized rubber," *International Journal of Solids and Structures*, vol. 185-186, pp. 365-379, 2020.

[12] A. Duda and S. Penczek, "Anionic copolymerisation of elemental sulfur with 2, 2-dimethylthiirane," *Die Makromolekulare Chemie: Macromolecular Chemistry and Physics*, vol. 181, no. 5, pp. 995-1001, 1980.

[13] S. Penczek, R. Ślazak, and A. Duda, "Anionic copolymerisation of elemental sulphur," *Nature*, vol. 273, no. 5665, pp. 738-739, 1978.

[14] L. B. Blight, B. R. Currell, B. J. Nash, T. M. Scott, and C. Stillo, "Chemistry of the modification of sulphur by the use of dicyclopentadiene and of styrene," *British Polymer Journal*, vol. 12, no. 1, pp. 5-11, 1980.

[15] T. Tsuda and A. Takeda, "Palladium-catalysed cycloaddition copolymerisation of diynes with elemental sulfur to poly (thiophene) s," *Chemical Communications*, no. 11, pp. 1317-1318, 1996.

[16] Y. Ding and A. S. Hay, "Copolymerization of elemental sulfur with cyclic (arylene disulfide) oligomers," *Journal of Polymer Science Part A: Polymer Chemistry*, vol. 35, no. 14, pp. 2961-2968, 1997.

[17] B. Meyer and N. Kharasch, *Elemental sulfur : chemistry and physics*. New York; London: Interscience, 1965.

[18] B. Meyer, "Elemental sulfur," *Chemical Reviews*, vol. 76, no. 3, pp. 367-388, 1976/06/01 1976.

[19] Y. Zhang *et al.*, "Inverse vulcanization of elemental sulfur and styrene for polymeric cathodes in Li-S batteries," *Journal of Polymer Science Part A: Polymer Chemistry*, vol. 55, no. 1, pp. 107-116, 2016.

[20] M. Arslan, B. Kiskan, and Y. Yagci, "Combining elemental sulfur with polybenzoxazines via inverse vulcanization," *Macromolecules*, vol. 49, no. 3, pp. 767-773, 2016.

[21] M. Armand and J.-M. Tarascon, "Building better batteries," *Nature*, vol. 451, no. 7179, pp. 652-657, 2008.

[22] Y.-J. Choi, Y.-D. Chung, C.-Y. Baek, K.-W. Kim, H.-J. Ahn, and J.-H. Ahn, "Effects of carbon coating on the electrochemical properties of sulfur cathode for lithium/sulfur cell," *Journal of Power Sources,* vol. 184, no. 2, pp. 548-552, 2008.

[23] B. L. Ellis, K. T. Lee, and L. F. Nazar, "Positive electrode materials for Li-ion and Li-batteries," *Chemistry of materials,* vol. 22, no. 3, pp. 691-714, 2010.

[24] N. Jayaprakash, J. Shen, S. S. Moganty, A. Corona, and L. A. Archer, "Porous hollow carbon@ sulfur composites for high-power lithium–sulfur batteries," *Angewandte Chemie International Edition,* vol. 50, no. 26, pp. 5904-5908, 2011.

[25] X. Ji, K. T. Lee, and L. F. Nazar, "A highly ordered nanostructured carbon–sulphur cathode for lithium–sulphur batteries," *Nature materials,* vol. 8, no. 6, pp. 500-506, 2009.

[26] Y. Kiya, A. Iwata, T. Sarukawa, J. C. Henderson, and H. D. Abruña, "Poly [dithio-2, 5-(1, 3, 4-thiadiazole)](PDMcT)–poly (3, 4-ethylenedioxythiophene)(PEDOT) composite cathode for high-energy lithium/lithium-ion rechargeable batteries," *Journal of Power Sources,* vol. 173, no. 1, pp. 522-530, 2007.

[27] M.-S. Song *et al.*, "Effects of nanosized adsorbing material on electrochemical properties of sulfur cathodes for Li/S secondary batteries," *Journal of the Electrochemical Society,* vol. 151, no. 6, pp. A791-95, 2004.

[28] H. Wang *et al.*, "Graphene-wrapped sulfur particles as a rechargeable lithium–sulfur battery cathode material with high capacity and cycling stability," *Nano letters,* vol. 11, no. 7, pp. 2644-2647, 2011.

[29] J. Wang, J. Yang, C. Wan, K. Du, J. Xie, and N. Xu, "Sulfur composite cathode materials for rechargeable lithium batteries," *Advanced Functional Materials,* vol. 13, no. 6, pp. 487-492, 2003.

[30] F. Wu *et al.*, "Sulfur/polythiophene with a core/shell structure: synthesis and electrochemical properties of the cathode for rechargeable lithium batteries," *The Journal of Physical Chemistry C,* vol. 115, no. 13, pp. 6057-6063, 2011.

[31] F. Wu, S. Wu, R. Chen, J. Chen, and S. Chen, "Sulfur–polythiophene composite cathode materials for rechargeable lithium batteries," *Electrochemical and Solid State Letters*, vol. 13, no. 4, p. A29, 2010.

[32] G. Yu *et al.*, "Enhancing the supercapacitor performance of graphene/MnO2 nanostructured electrodes by conductive wrapping," *Nano letters*, vol. 11, no. 10, pp. 4438-4442, 2011.

[33] J.-g. Liu and M. Ueda, "High refractive index polymers: fundamental research and practical applications," *Journal of Materials Chemistry*, vol. 19, no. 47, pp. 8907-8919, 2009.

[34] R. Okutsu, S. Ando, and M. Ueda, "Sulfur-containing poly (meth) acrylates with high refractive indices and high Abbe's numbers," *Chemistry of Materials*, vol. 20, no. 12, pp. 4017-4023, 2008.

[35] C. Almeida, H. Costa, P. Kadhirvel, A. Queiroz, R. Dias, and M. Costa, "Electrochemical activity of sulfur networks synthesized through RAFT polymerization," *Journal of Applied Polymer Science*, vol. 133, no. 39, 2016.

[36] P. T. Dirlam *et al.*, "Elemental sulfur and molybdenum disulfide composites for Li–S batteries with long cycle life and high-rate capability," *ACS applied materials & interfaces*, vol. 8, no. 21, pp. 13437-13448, 2016.

[37] J. J. Griebel *et al.*, "Preparation of dynamic covalent polymers via inverse vulcanization of elemental sulfur," *ACS Macro Letters*, vol. 3, no. 12, pp. 1258-1261, 2014.

[38] G. Hu *et al.*, "A sulfur-rich copolymer@ CNT hybrid cathode with dual-confinement of polysulfides for high-performance lithium–sulfur batteries," *Advanced materials*, vol. 29, no. 11, p. 1603835, 2017.

[39] B. Li, S. Li, J. Xu, and S. Yang, "A new configured lithiated silicon–sulfur battery built on 3D graphene with superior electrochemical performances," *Energy & Environmental Science*, vol. 9, no. 6, pp. 2025-2030, 2016.

[40] Y. Wei *et al.*, "Solution processible hyperbranched inverse-vulcanized polymers as new cathode materials in Li–S batteries," *Polymer Chemistry*, vol. 6, no. 6, pp. 973-982, 2015.

[41] V. S. Wadi, K. K. Jena, S. Z. Khawaja, V. M. Ranagraj, and Saeed M. Alhassan, "Preparation and processing of porous sulfur foams having low thermal conductivity," *RSC Advances,* vol. 9, no. 8, pp. 4397-4403, 2019.

[42] W. J. Chung *et al.*, "Elemental sulfur as a reactive medium for gold nanoparticles and nanocomposite materials," *Angewandte Chemie International Edition,* vol. 123, no. 48, pp. 11611-11614, 2011.

[43] I. Gomez *et al.*, "Inverse vulcanization of sulfur with divinylbenzene: Stable and easy processable cathode material for lithium-sulfur batteries," *Journal of Power Sources,* vol. 329, pp. 72-78, 2016.

[44] M. K. Salman, B. Karabay, L. C. Karabay, and A. Cihaner, "Elemental sulfur-based polymeric materials: Synthesis and characterization," *Journal of Applied Polymer Science,* vol. 133, no. 28, 2016.

[45] H. Berk, B. Balci, S. Ertan, M. Kaya, and A. Cihaner, "Functionalized polysulfide copolymers with 4-vinylpyridine via inverse vulcanization," *Materials Today Communications,* vol. 19, pp. 336-341, 2019.

[46] M. P. Crockett *et al.*, "Sulfur-Limonene Polysulfide: A Material Synthesized Entirely from Industrial By-Products and Its Use in Removing Toxic Metals from Water and Soil," *Angewandte Chemie International Edition,* vol. 55, no. 5, pp. 1714-1718, 2016.

[47] I. Gomez, O. Leonet, J. A. Blazquez, and D. Mecerreyes, "Inverse vulcanization of sulfur using natural dienes as sustainable materials for lithium–sulfur batteries," *ChemSusChem,* vol. 9, no. 24, pp. 3419-3425, 2016.

[48] D. Parker *et al.*, "Low cost and renewable sulfur-polymers by inverse vulcanisation, and their potential for mercury capture," *Journal of Materials Chemistry A,* vol. 5, no. 23, pp. 11682-11692, 2017.

[49] K. Yamabuki, K. Itaoka, T. Shinchi, N. Yoshimoto, K. Ueno, and H. Tsutsumi, "Soluble sulfur-based copolymers prepared from elemental sulfur and alkenyl alcohol as positive active material for lithium-sulfur batteries," *Polymer,* vol. 117, pp. 225-230, 2017.

[50] T. R. Martin, K. A. Mazzio, H. W. Hillhouse, and C. K. Luscombe, "Sulfur copolymer for the direct synthesis of ligand-free CdS nanoparticles," *Chemical Communications,* vol. 51, no. 56, pp. 11244-11247, 2015.

[51] M. Arslan, B. Kiskan, E. C. Cengiz, R. Demir-Cakan, and Y. Yagci, "Inverse vulcanization of bismaleimide and divinylbenzene by elemental sulfur for lithium sulfur batteries," *European Polymer Journal,* vol. 80, pp. 70-77, 2016.

[52] S. Shukla, A. Ghosh, U. K. Sen, P. K. Roy, S. Mitra, and B. Lochab, "Cardanol benzoxazine-Sulfur Copolymers for Li-S batteries: Symbiosis of Sustainability and Performance," *ChemistrySelect,* vol. 1, no. 3, pp. 594-600, 2016.

[53] T. S. Kleine *et al.*, "High refractive index copolymers with improved thermomechanical properties via the inverse vulcanization of sulfur and 1, 3, 5-triisopropenylbenzene," *ACS Macro Letters,* vol. 5, no. 10, pp. 1152-1156, 2016.

[54] A. Hoefling, D. T. Nguyen, Y. J. Lee, S.-W. Song, and P. Theato, "A sulfur–eugenol allyl ether copolymer: a material synthesized via inverse vulcanization from renewable resources and its application in Li–S batteries," *Materials Chemistry Frontiers,* vol. 1, no. 9, pp. 1818-1822, 2017.

[55] A. Hoefling, Y. J. Lee, and P. Theato, "Sulfur-Based Polymer Composites from Vegetable Oils and Elemental Sulfur: A Sustainable Active Material for Li-S Batteries," *Macromolecular Chemistry and Physics,* vol. 218, no. 1, 2017.

[56] N. A. Lundquist *et al.*, "Polysulfides made from re-purposed waste are sustainable materials for removing iron from water," *RSC advances,* vol. 8, no. 3, pp. 1232-1236, 2018.

[57] Z. Sun *et al.*, "Sulfur-rich polymeric materials with semi-interpenetrating network structure as a novel lithium–sulfur cathode," *Journal of materials chemistry A,* vol. 2, no. 24, pp. 9280-9286, 2014.

[58] P. T. Dirlam *et al.*, "Inverse vulcanization of elemental sulfur with 1, 4-diphenylbutadiyne for cathode materials in Li–S batteries," *Rsc Advances,* vol. 5, no. 31, pp. 24718-24722, 2015.

[59] S. Z. Khawaja, S. Vijay Kumar, K. K. Jena, and S. M. Alhassan, "Flexible sulfur film from inverse vulcanization technique," *Materials Letters,* vol. 203, pp. 58-61, 2017.

[60] E. T. Kim *et al.*, "One-pot synthesis of PbS NP/sulfur-oleylamine copolymer nanocomposites via the copolymerization of elemental sulfur with oleylamine," *Polymer Chemistry,* vol. 5, no. 11, pp. 3617-3623, 2014.

[61] K. C. Nicolaou, P. G. Bulger, and D. Sarlah, "Palladium-catalyzed cross-coupling reactions in total synthesis," *Angewandte Chemie International Edition,* vol. 44, no. 29, pp. 4442-4489, 2005.

[62] C. Torborg, M. Beller, and Catalysis, "Recent applications of palladium-catalyzed coupling reactions in the pharmaceutical, agrochemical, and fine chemical industries," *Advanced Synthesis,* vol. 351, no. 18, pp. 3027-3043, 2009.

[63] C. Barbante *et al.*, "Greenland snow evidence of large scale atmospheric contamination for platinum, palladium, and rhodium," *Environmental science & technology,* vol. 35, no. 5, pp. 835-839, 2001.

[64] K. C. Galbreath and C. J. Zygarlicke, "Mercury transformations in coal combustion flue gas," *Fuel Processing Technology,* vol. 65, pp. 289-310, 2000.

[65] O. Malm, "Gold mining as a source of mercury exposure in the Brazilian Amazon," *Environmental research,* vol. 77, no. 2, pp. 73-78, 1998.

[66] S. M. Wilhelm and N. Bloom, "Mercury in petroleum," *Fuel Processing Technology,* vol. 63, no. 1, pp. 1-27, 2000.

[67] P. B. Tchounwou, W. K. Ayensu, N. Ninashvili, and D. Sutton, "Environmental exposure to mercury and its toxicopathologic implications for public health," *Environmental Toxicology: An International Journal,* vol. 18, no. 3, pp. 149-175, 2003.

[68] D. R. Vardon *et al.*, "Hydrothermal catalytic processing of saturated and unsaturated fatty acids to hydrocarbons with glycerol for in situ hydrogen production," *Green Chemistry,* vol. 16, no. 3, pp. 1507-1520, 2014.

[69] C. Byrne, G. Subramanian, and S. C. Pillai, "Recent advances in photocatalysis for environmental applications," *Journal of Environmental Chemical Engineering,* vol. 6, no. 3, pp. 3531-3555, 2018.

[70] U. I. Gaya and A. H. Abdullah, "Heterogeneous photocatalytic degradation of organic contaminants over titanium dioxide: a review of fundamentals, progress and problems," *Journal of photochemistry photobiology C: Photochemistry reviews,* vol. 9, no. 1, pp. 1-12, 2008.

[71] K. Kabra, R. Chaudhary, and R. L. Sawhney, "Treatment of hazardous organic and inorganic compounds through aqueous-phase photocatalysis: a review," *Industrial & engineering chemistry research,* vol. 43, no. 24, pp. 7683-7696, 2004.

[72] F. Meng, F. Lu, Z. Sun, and J. Lü, "A mechanism for enhanced photocatalytic activity of nano-size silver particle modified titanium dioxide thin films," *Science China Technological Sciences,* vol. 53, no. 11, pp. 3027-3032, 2010.

[73] X. Guan, J. Chang, Z. Xu, Y. Chen, and H. Fan, "Remediation of chromium (iii)-contaminated tannery effluents by using gallic acid-conjugated magnetite nanoparticles," *RSC advances,* vol. 6, no. 35, pp. 29054-29063, 2016.

[74] M. N. Chong, B. Jin, C. W. Chow, and C. Saint, "Recent developments in photocatalytic water treatment technology: a review," *Water research,* vol. 44, no. 10, pp. 2997-3027, 2010.

[75] D. Wang *et al.,* "Mechanism and experimental study on the photocatalytic performance of Ag/AgCl@ chiral TiO2 nanofibers photocatalyst: The impact of wastewater components," *Journal of hazardous materials,* vol. 285, pp. 277-284, 2015.

[76] K. Nakata and A. Fujishima, "TiO2 photocatalysis: Design and applications," *Journal of Photochemistry and Photobiology C: Photochemistry Reviews,* vol. 13, no. 3, pp. 169-189, 2012.

[77] R. Liang, A. Hu, M. Hatat-Fraile, and N. Zhou, "Development of TiO2 Nanowires for Membrane Filtration Applications," in *Nanotechnology for Water Treatment and Purification*, A. Hu and A. Apblett, Eds. Cham: Springer International Publishing, 2014, pp. 47-77.

[78] S. Min, F. Wang, and Y. Han, "An investigation on synthesis and photocatalytic activity of polyaniline sensitized nanocrystalline TiO2 composites," *Journal of Materials Science,* vol. 42, no. 24, pp. 9966-9972, 2007/12/01 2007.

[79] F. Wang, S. Min, Y. Han, and L. Feng, "Visible-light-induced photocatalytic degradation of methylene blue with polyaniline-sensitized TiO2 composite photocatalysts," *Superlattices and Microstructures,* vol. 48, no. 2, pp. 170-180, 2010.

[80] J. Ge, Y. Zhang, Y.-J. Heo, and S.-J. Park, "Advanced design and synthesis of composite photocatalysts for the remediation of wastewater: A review," *Catalysts,* vol. 9, no. 2, p. 122, 2019.

[81] J. Gómez-Pastora, S. Dominguez, E. Bringas, M. J. Rivero, I. Ortiz, and D. D. Dionysiou, "Review and perspectives on the use of magnetic nanophotocatalysts (MNPCs) in water treatment," *Chemical Engineering Journal,* vol. 310, pp. 407-427, 2017.

[82] L. Mohammed, H. G. Gomaa, D. Ragab, and J. Zhu, "Magnetic nanoparticles for environmental and biomedical applications: A review," *Particuology,* vol. 30, pp. 1-14, 2017.

[83] Y. Zhang *et al.,* "Nanomaterials-enabled water and wastewater treatment," *NanoImpact,* vol. 3, pp. 22-39, 2016.

[84] D. Stanicki, L. Vander Elst, R. N. Muller, and S. Laurent, "Synthesis and processing of magnetic nanoparticles," *Current Opinion in Chemical Engineering,* vol. 8, pp. 7-14, 2015.

[85] A. Parma *et al.,* "Structural and magnetic properties of mesoporous SiO 2 nanoparticles impregnated with iron oxide or cobalt-iron oxide nanocrystals," *Journal of Materials Chemistry,* vol. 22, no. 36, pp. 19276-19288, 2012.

[86] S. Teixeira *et al.,* "Photocatalytic degradation of recalcitrant micropollutants by reusable Fe3O4/SiO2/TiO2 particles," *Journal of Photochemistry and Photobiology A: Chemistry,* vol. 345, pp. 27-35, 2017.

[87] C.-C. Wang and J. Y. Ying, "Sol− gel synthesis and hydrothermal processing of anatase and rutile titania nanocrystals," *Chemistry of materials,* vol. 11, no. 11, pp. 3113-3120, 1999.

[88] T. Rashid, D. Iqbal, A. Hazafa, S. Hussain, F. Sher, and F. Sher, "Formulation of zeolite supported nano-metallic catalyst and applications in textile effluent treatment," *Journal of Environmental Chemical Engineering,* vol. 8, no. 4, p. 104023, 2020.

[89] M. S. Kumar, S. Sonawane, and A. B. Pandit, "Degradation of methylene blue dye in aqueous solution using hydrodynamic cavitation based hybrid advanced oxidation processes," *Chemical Engineering and Processing: Process Intensification,* vol. 122, pp. 288-295, 2017.

[90] A. Lincy, P. Jegathambal, M. Mkandawire, and S. MacQuarrie, "Nano bioremediation of textile dye effluent using magnetite nanoparticles encapsulated alginate beads," *Journal of Environmental Treatment Techniques,* vol. 8, no. 3, pp. 936-946, 2020.

[91] M. Muniyandi and P. Govindaraj, "Potential removal of Methylene Blue dye from synthetic textile effluent using activated carbon derived from Palmyra (Palm) shell," *Materials Today: Proceedings,* 2021.

[92] U. Mahanta, M. Khandelwal, and A. S. Deshpande, "TiO2@ SiO2 nanoparticles for methylene blue removal and photocatalytic degradation under natural sunlight and low-power UV light," *Applied Surface Science,* vol. 576, p. 151745, 2022.

[93] S. Manna, D. Roy, P. Saha, D. Gopakumar, and S. Thomas, "Rapid methylene blue adsorption using modified lignocellulosic materials," *Process Safety and Environmental Protection,* vol. 107, pp. 346-356, 2017.

[94] A. K. Moorthy, B. G. Rathi, S. P. Shukla, K. Kumar, and V. S. Bharti, "Acute toxicity of textile dye Methylene blue on growth and metabolism of selected freshwater microalgae," *Environmental Toxicology and Pharmacology,* vol. 82, p. 103552, 2021.

[95] M. R. Ladole, P. B. Pokale, S. S. Patil, P. G. Belokar, and A. B. Pandit, "Laccase immobilized peroxidase mimicking magnetic metal organic frameworks for industrial dye degradation," *Bioresource Technology,* vol. 317, p. 124035, 2020.

[96] B. Bharati, A. Sonkar, N. Singh, D. Dash, and C. Rath, "Enhanced photocatalytic degradation of dyes under sunlight using biocompatible TiO2 nanoparticles," *Materials Research Express,* vol. 4, no. 8, p. 085503, 2017.

[97] M. T. Amin and A. A. Alazba, "Structural study of monoclinic TiO2 nanostructures and photocatalytic applications for degradation of crystal violet dye," *Modern Physics Letters B,* vol. 31, no. 29, p. 1750264, 2017.

[98] G. G. Bessegato, J. C. Cardoso, and M. V. B. Zanoni, "Enhanced photoelectrocatalytic degradation of an acid dye with boron-doped TiO2 nanotube anodes," *Catalysis Today*, vol. 240, pp. 100-106, 2015.

[99] R. A. Putri, S. Safni, N. Jamarun, U. Septiani, M.-K. Kim, and K.-D. Zoh, "Degradation and mineralization of violet-3B dye using CN-codoped TiO 2 photocatalyst," *Environmental Engineering Research*, vol. 25, no. 4, pp. 529-535, 2020.

[100] I. Ali, O. M. Alharbi, Z. A. Alothman, and A. Y. Badjah, "Kinetics, thermodynamics, and modeling of amido black dye photodegradation in water using Co/TiO2 nanoparticles," *Photochemistry and Photobiology*, vol. 94, no. 5, pp. 935-941, 2018.

[101] Y. Zhang *et al.*, "Non-uniform doping outperforms uniform doping for enhancing the photocatalytic efficiency of Au-doped TiO2 nanotubes in organic dye degradation," *Ceramics International*, vol. 43, no. 12, pp. 9053-9059, 2017.

[102] Z.-H. Ren *et al.*, "Au nanoparticles embedded on urchin-like TiO2 nanosphere: an efficient catalyst for dyes degradation and 4-nitrophenol reduction," *Materials & Design*, vol. 121, pp. 167-175, 2017.

[103] B. Pal, R. Kaur, and I. S. Grover, "Superior adsorption and photodegradation of eriochrome black-T dye by Fe3+ and Pt4+ impregnated TiO2 nanostructures of different shapes," *Journal of Industrial and Engineering Chemistry*, vol. 33, pp. 178-184, 2016.

[104] F. Han, V. Kambala, R. Dharmarajan, Y. Liu, and R. Naidu, "Photocatalytic degradation of azo dye acid orange 7 using different light sources over Fe3+-doped TiO2 nanocatalysts," *Environmental Technology & Innovation*, vol. 12, pp. 27-42, 2018.

[105] U. O. Bhagwat, J. J. Wu, A. M. Asiri, and S. Anandan, "Sonochemical Synthesis of Mg-TiO2 nanoparticles for persistent Congo red dye degradation," *Journal of Photochemistry and Photobiology A: Chemistry*, vol. 346, pp. 559-569, 2017.

[106] Z. Dai *et al.*, "Preparation of porphyrin sensitized three layers magnetic nanocomposite Fe3O4@ SiO2@ TiO2 as an efficient photocatalyst," *Materials Letters*, vol. 241, pp. 239-242, 2019.

[107] M. A. Habila, Z. A. ALOthman, A. M. El-Toni, J. P. Labis, and M. Soylak, "Synthesis and application of Fe3O4@ SiO2@ TiO2 for photocatalytic decomposition of organic matrix simultaneously with magnetic solid phase extraction of heavy metals prior to ICP-MS analysis," *Talanta,* vol. 154, pp. 539-547, 2016.

[108] A. Pourzad, H. R. Sobhi, M. Behbahani, A. Esrafili, R. R. Kalantary, and M. Kermani, "Efficient visible light-induced photocatalytic removal of paraquat using N-doped TiO2@ SiO2@ Fe3O4 nanocomposite," *Journal of Molecular Liquids,* vol. 299, p. 112167, 2020.

[109] W. Szeto, J. Li, H. Huang, J. Xuan, and D. Y. Leung, "Novel urchin-like Fe 2 O 3@ SiO 2@ TiO 2 microparticles with magnetically separable and photocatalytic properties," *RSC Advances,* vol. 5, no. 68, pp. 55363-55371, 2015.

[110] X. Lv *et al.*, "Preparation and photocatalytic activity of Fe3O4@ SiO2@ ZnO: La," *Journal of Rare Earths,* vol. 38, no. 12, pp. 1288-1296, 2020.

[111] Q.-Y. Li *et al.*, "Preparation and enhanced photocatalytic performance of a novel photocatalyst: hollow network Fe3O4/mesoporous SiO2/TiO2 (FST) composite microspheres," *Microporous and Mesoporous Materials,* vol. 265, pp. 18-25, 2018.